NASA TN D-31

TECHNICAL NOTE
D-31

A DYNAMIC MODEL INVESTIGATION OF THE EFFECT OF A SHARP-EDGE VERTICAL GUST ON BLADE PERIODIC FLAPPING ANGLES AND BENDING MOMENTS OF A TWO-BLADE ROTOR

By John Locke McCarty, George W. Brooks,
and Domenic J. Maglieri

Langley Research Center
Langley Field, Va.

NATIONAL AERONAUTICS AND SPACE ADMINISTRATION

WASHINGTON September 1959

NATIONAL AERONAUTICS AND SPACE ADMINISTRATION

TECHNICAL NOTE D-31

A DYNAMIC MODEL INVESTIGATION OF THE EFFECT OF A SHARP-EDGE VERTICAL GUST ON BLADE PERIODIC FLAPPING ANGLES AND BENDING MOMENTS OF A TWO-BLADE ROTOR

By John Locke McCarty, George W. Brooks,
and Domenic J. Maglieri

SUMMARY

A two-blade rotor having a diameter of 4 feet and a solidity of 0.037 was subjected to sharp-edge vertical gusts while being operated at various forward speeds to study the effect of the gusts on the blade periodic bending moments and flapping angles. Variables studied included gust velocity, collective pitch angle, flapping hinge offset, and tip-speed ratio.

Dimensionless coefficients are derived for the periodic components of the incremental changes in blade flapping angles and bending moments which arise when a rotor blade penetrates a sharp-edge gust. The incremental changes in both the flapping angles and bending moments are essentially proportional to gust velocity, and the coefficients express the ratio of these increments to gust velocity. The results show that the flapping coefficient usually increases with an increase in collective pitch angle, is generally dependent on tip-speed ratio, and is essentially independent of the amount of flapping hinge offset.

The bending-moment coefficient is also dependent on collective pitch angle and tip-speed ratio. Expected reductions in bending moments are realized by the use of flapping hinges, and further reductions in bending moments are achieved as the amount of flapping hinge offset is increased.

Comparison of the experimental results of this investigation with limited available theoretical results shows substantial agreement but indicates that the assumption that the response of the rotor to a sharp-edge gust is independent of the collective pitch angle prior to gust entry is probably inadequate.

INTRODUCTION

The effects of atmospheric turbulence on the loads and stresses of helicopters have been of concern for many years, and a considerable amount of effort has been devoted to an assessment of the subject. References 1 and 2 present flight-test measurements of the normal rigid-body accelerations of helicopters resulting from maneuvers and from flights in gusty air. Reference 3 presents the results of a flight investigation of the effects of turbulence and maneuvers on the blade periodic flapwise bending and torsional moments. This study, performed on a specific helicopter configuration, indicated no significant increase in the total blade bending moments due to turbulence or moderate pullup maneuvers which produced center-of-gravity acceleration increments of less than about 0.15g (where g is the acceleration due to gravity). Flight-test conditions resulting in higher center-of-gravity acceleration, however, indicated that the blade flapwise bending moments were increased, particularly in the higher harmonics. Reference 4 presents the results of tower tests of a full-scale rotor operating in gusty air wherein the high bending moments associated with the prevailing velocity of the wind past the tower were combined with the bending moments due to the gust in such a way that the isolated effects due to the gust could not be determined.

In order to isolate and study the gust effects, a preliminary experimental investigation of the effects of sharp-edge vertical gusts on the flapwise bending moments of small two-blade teetering and fixed-at-root rotor models was made in the Langley gust tunnel and the results are given in reference 5.

A comprehensive analytical procedure for the calculation of the effects of gusts on both the overall helicopter response and the response of the blades is given in reference 6. Even with several simplifying assumptions the analysis still involves an extensive step-by-step numerical procedure, and only a few cases have been analyzed to determine the blade bending moments and flapping angles.

In an effort to extend the previous model studies to more useful configurations and to cover a wider range of operating variables, and in an effort to derive overall parameters which might provide suitable criteria for comparison of measured blade bending moments and flapping angles with some analytical results of reference 6, an experimental investigation of several two-blade rotor configurations was made and the results are reported herein. Tests were made by mounting small rotor models on the end of a horizontal whirling arm so that the rotor passed through a sharp-edge gust during each revolution of the whirling arm. The transient response of the blades due to the penetration of the sharp-edge gusts by the rotor is presented in terms of appropriate nondimensional blade flapping angle and bending-moment parameters.

Although the sharp-edge gust is probably not a realistic representation of atmospheric conditions, it does provide some means of comparison of theoretical and experimental results and provides a suitable basis for studying effects of rotor parameters on the blade response during turbulent atmospheric conditions.

SYMBOLS

f, f_1, g, g_1	functional notation
e	distance from flapping hinge to axis of rotation, ft unless otherwise stated
M_o	double amplitude of blade periodic flapwise bending motion, measured with rotor operating in smooth air, in-lb
M	maximum double amplitude of blade periodic flapwise bending moment, measured as rotor penetrates a gust, in-lb
ΔM	transient gust effect on double amplitude of blade periodic flapwise bending moment, $M - M_o$, in-lb
r	radial distance to blade element, ft unless otherwise stated
R	blade radius, ft unless otherwise stated
V	airspeed of rotor along flight path, fps
U	gust velocity, fps
EI	blade flapwise bending stiffness, $lb\text{-}in^2$
$\bar{\beta}_o$	double amplitude of blade periodic flapping angle, measured with rotor operating in smooth air, deg
$\bar{\beta}$	maximum double amplitude of blade periodic flapping angle, measured as rotor penetrates a gust, deg
$\Delta\bar{\beta}$	transient gust effect on double amplitude of blade periodic flapping angle, $\bar{\beta} - \bar{\beta}_o$, deg
θ	blade collective pitch angle, deg
μ	tip-speed ratio, $V \cos \alpha / R\Omega$ ($\cos \alpha$ assumed equal to 1, where α is the rotor angle of attack)

Ω	rotor angular velocity, radians/sec
ψ	blade azimuth angle, deg
C_T	rotor thrust coefficient, $\frac{\text{Thrust}}{\pi R^2(R\Omega)^2\rho}$
ρ	mass density of air, slug/cu ft
$B_{\Delta\overline{\beta}}$	incremental flapping coefficient
$B_{\Delta M}$	incremental bending-moment coefficient
γ	Lock number (see appendix)

Subscript:

max	maximum

APPARATUS AND TESTS

Apparatus

The apparatus used in these tests consisted of a rotor assembly which was attached to the end of a whirling arm. This position caused the rotor to pass through the open jet of the Langley gust tunnel. Photographs of the test apparatus are presented in figures 1 and 2 and a sketch showing the appropriate overall dimensions of the apparatus is given in figure 3.

Rotor characteristics and configurations.- The rotor configurations studied in this investigation consisted of two-blade rotors attached to the shaft by means of various blade root fittings, each root fitting defining a configuration. Tests were performed on configurations with flapping hinges having offsets of 0, 5, and 10 percent of the rotor radius and, as a matter of comparative interest, tests were also made on a fixed-at-root (cantilever) configuration. Sketches of the blade root fittings are given in figures 4 and 5. Figure 4 describes the fixed-at-root configuration. The configuration shown in figure 5 corresponds to the 5-percent flapping hinge offset condition ($e/R = 0.05$); however, the offset fittings for the other flapping configurations were similarly constructed by varying the lengths of both the hub and the extension plates. Drag hinges, noted on the figures by the drag hinge pin, were used in all configurations and were located at $r/R = 0.15$. Drag hinge dampers for in-plane motion, however, were used only on the flapping configurations.

As indicated in figure 5, blade retention straps were provided in the flapping configurations to transmit the centrifugal forces to the hub. A change in blade offset was accomplished by removing the drag hinge pin and installing the desired hub assembly. Figure 5 shows that the blade collective pitch angle would be unaffected by changes in the offset fitting since the provisions to change the pitch angle were located outboard of the drag hinge pin.

All configurations had a rotor diameter of 4 feet and a solidity of 0.037. The blades were untwisted, rectangular in plan form with a chord of 1.4 inches, and had an NACA 0012 airfoil section. The blades were scaled in stiffness and weight to possess the dynamic characteristics representative of present-day helicopter blades. This scaling was accomplished by constructing an aluminum spar having the proper weight and stiffness distributions and a cellulose acetate material was then molded on the spar to form the blade profile.

The stiffness and weight distributions along the span are given in figures 6 and 7, respectively, for the various configurations. Frequency diagrams for the blade in each of the four configurations are presented in figure 8 in which the uncoupled natural frequencies of the first three bending modes are plotted, together with harmonics of the rotor frequency, as functions of the rotor speed. The natural frequencies of the nonrotating blade were measured experimentally, and the natural frequencies of the rotating blade were determined by using the procedure of reference 7. The rotor speed, held constant during these tests, is indicated on the figure by the vertical line.

Whirling arm.- The rotor assembly was rigidly attached to the end of a rotating arm (radius, 15 feet) hereinafter referred to as the "whirling arm" which was rotated in a horizontal plane and restrained in vertical motion. (See figs. 1 and 3.) Forward speed of the rotor was attained by rotating the whirling arm which was mounted adjacent to the test section of the Langley gust tunnel such that, during the course of rotation, the model passed over the jet. (See fig. 3.)

Tunnel characteristics.- The Langley gust tunnel (ref. 8) is an open-throat low-velocity tunnel producing an 8- by 14-foot vertical jet of air. The velocity profile in the plane of the rotor is approximately rectangular in shape as shown in figure 9.

Instrumentation

One blade of the rotor was instrumented to measure the blade flapping angles and the blade bending motions. The blade flapping angles were measured by means of the electrical-resistance-wire flapping indicator shown in figure 5. The blade bending motions were measured by strain-gage

bridges mounted to the spar at four spanwise stations (r/R = 0.25, 0.42, 0.625, and 0.833). Calibration of the blade consisted of static tests which involved deflecting the blade through a range of known angles for flapping and the application of known weights to the blade tip for the bending moments. The periodic variation of rotor thrust was also measured and was obtained from a strain-gage bridge mounted on the rotor balance which is indicated in figure 3. Bridges were also mounted on the rotor balance to indicate hub moments but these were not used during this investigation.

A rotor speed timer was used to record the speed of the rotor. The rotor speed was set at the beginning of each test by regulating the voltage to the drive motor and was checked by means of a stroboscopic light.

The forward speed of the rotor was measured by means of a microswitch located on the hub of the whirling arm. A slipring brush assembly, mounted on the rotor shaft in a housing as shown in figures 1 to 3, was used to transmit the signals from the rotor to the control station. These signals were recorded by an oscillograph together with the signals from the forward speed indicator. A sample oscillograph record is shown in figure 10 and is discussed in a subsequent section.

Model Scale Factors

As previously mentioned, the blades were scaled in both stiffness and weight to be representative of the dynamic characteristics of present-day helicopter blades. The following table gives some pertinent structural characteristics and the range of test conditions of the model together with the corresponding values for a representative full-scale rotor of 24-foot radius when both are assumed to be operating at the same lift coefficient and tip-speed ratio.

Characteristic	Model value	Scale factor	Equivalent full-scale value
Blade bending stiffness, EI, $lb\text{-}in^2$	78	12^5	19,409,000
Blade weight, lb/in.	0.00409	12^2	0.589
Rotor radius, ft	2	12	24
Rotor speed, rpm	800	$1/\sqrt{12}$	231
Tip speed, fps	166.5	$\sqrt{12}$	577
Forward velocity, fps	0 to 46.7	$\sqrt{12}$	0 to 161.8
Tip-speed ratio	0 to 0.28	1	0 to 0.28
Gust velocity, fps	5; 7.5; 10	$\sqrt{12}$	17.3; 26; 34.6

Whereas the flapping angles of the equivalent full-scale rotor would be identical to those measured on the model, the full-scale bending moments would be obtained by multiplying the model values by 12^4.

Test Procedure

Testing technique.- The testing technique involved the rotation of the whirling arm such that the rotor, operating at the test value of 800 revolutions per minute, penetrated a preset gust at various forward speeds. Oscillograph records were taken of the strain-gage responses prior to and during penetration of the gust by the rotor.

All the configurations were tested over a range of forward speeds at a rotor angle of attack of zero. Data were taken with the configurations operating under forward-flight conditions both without gusts and when subjected to sharp-edge vertical gusts of 5, 7.5, and 10 feet per second.

No cyclic pitch was applied to the rotors during the tests; however, each of the configurations was tested at collective pitch angles of 0.6°, 3.4°, and 6.6°. In order to minimize the errors associated with changes in blade collective pitch angle, all tests associated with one pitch angle were concluded before repeating the test procedure for a different pitch-angle setting.

Determination of collective pitch angle.- The collective pitch angles for the tests were nominally set by means of a protractor, but the effective values, used to designate the different test conditions presented in this paper, were obtained from measurements of the static thrust. The thrust was then calculated at the various forward speeds and compared on the basis of rotor thrust coefficient with the measured values in figure 11 to determine whether the collective pitch angle derived from the hovering thrust data would yield thrust values compatible with those measured during forward-flight conditions. The results presented in figure 11 show that this is essentially the case for $\theta = 0.6^\circ$ and $\theta = 3.4^\circ$; however, significant differences are apparent for $\theta = 6.6^\circ$ at the higher values of μ. No allowances were made for the effects of stall for the calculated curves of C_T; however, there is considerable evidence that stall does occur and is primarily responsible for the differences in the C_T curves for $\theta = 6.6^\circ$. Reference 9 suggests that, for the Reynolds number of these blades (approximately 63,000 based on chord and the mean velocity at $R/2$), the stall angle is approximately 8°. Calculations by the methods of reference 10 indicate that, at $\theta = 6.6^\circ$, the stall angle at $\psi = 270^\circ$ is reached at the blade tip when $\mu = 0.118$ and moves inboard to the midspan station ($r/R = 0.5$) when μ is increased to 0.139.

METHOD OF ANALYSIS AND PRESENTATION

A typical time-history record taken during a test run is given in figure 10 which presents the responses of the four radially located blade bending-moment gages, the flapping-angle indicator, the thrust gage, and the timing devices. The relative position of the rotor with respect to the gust is given by the sketches in the lower part of the figure. Three salient features characterize the sample time history. The first of these is the steady-state periodic response of bending moments and flapping angles which occur prior to entry of the rotor into the gust. This response is a result of the forward speed of the rotor. The second feature is the transient response which occurs during and persists for a time after entry of the rotor into the gust. In this condition, the response is due to the combined effects of the transient nature of the aerodynamic loading and an increase in the rotor angle of attack. The third feature is a new steady-state condition which follows the entry transient and may or may not become completely established, depending upon the forward speed of the rotor. This flight condition is a result of the rotor operating at an angle of attack produced by the gust in conjunction with the forward speed of the rotor and only becomes established at low values of tip-speed ratio. At the higher forward speeds of the rotor there is insufficient time for the entry transient to decay before the exit of the rotor. The effect of changes in rotor angle of attack on the periodic bending-moment and flapping-angle responses are treated in reference 11.

As the rotor leaves the gust, another transient arises but, for the purposes of this paper, only the bending moments and flapping angles which result from the initial penetration of the rotor in the gust (entry transient), together with the corresponding pre-gust condition, are analyzed.

The procedure followed in the analysis of the data to obtain the blade periodic flapping angles and bending moments is described as follows: The double amplitude of the envelope of the blade-flapping trace deflections and the trace deflections of the blade strains were measured just prior to gust entry (no gust) and at the point of maximum response during gust penetration (gust).

The data points shown in figure 12 are typical of the results and show the double amplitude of the blade periodic flapping angles and the bending moments at a selected radial location as a function of tip-speed ratio. The procedure of running all three gust conditions consecutively for each rotor configuration yielded three times as many test points for the pre-gust condition as for the individual gust condition.

With regard to the scatter of the data for the transient gust effects, two factors are worthy of mention. In the first place, the problem is to

some extent statistical in nature due to the existence of some turbulence in the testing area due to successive rotations of the whirling arm and the circulation set up by the rotor-induced flow. Secondly, the magnitudes of the flapping angles and bending moments of the blades resulting from gust penetration are dependent to some extent on the azimuth of the blade when the blade tip first enters the gust. This is a random effect since, in a given run, it is very unlikely that the azimuth angle of the blade would be the same on successive passages of the rotor over the gust.

In order to tabulate the data for the many test conditions and parameters studied, it was necessary to fair curves through the data inasmuch as the value of tip-speed ratio at which the rotor intercepted the gust was subjected to considerable variation during successive rotations of the whirling arm. This fairing presented a problem because of the amount of scatter involved and the comparatively small number of test points from a statistical viewpoint. It was concluded that a curve of the visual mean of the data points would be representative. Such curves were then faired through the data points for the different configurations as illustrated in figure 12 and these were read at specific values of tip-speed ratio μ. These data are presented in tables I to IV.

The tables include the maximum double-amplitude blade flapping angle $\overline{\beta}$ and bending moments M at the four blade radial stations which occur during gust penetration. The tables also include the actual transient gust effects, designated by $\Delta\overline{\beta}$ and ΔM, for flapping angles and bending moments, respectively, which result from the combined effects of the transient nature of the aerodynamic loading and the change in rotor angle of attack, and are obtained by subtracting the forward-flight or no-gust response from the transient response.

Dimensionless parameters for the incremental changes in the periodic blade flapping angles and periodic blade bending moments which result when the rotor intercepts a sharp-edge gust are derived in the appendix. These parameters are designated as $B_{\Delta\overline{\beta}}$ and $B_{\Delta M}$, respectively, and are defined in the appendix by the expressions $B_{\Delta\overline{\beta}} = \dfrac{\Delta\overline{\beta}}{U/\Omega R}$ and $B_{\Delta M} = \dfrac{\Delta M}{U(\Omega R)\rho R^2 c}$.

DISCUSSION OF RESULTS

Blade Flapping Angles

The incremental flapping angles measured during the investigation, are presented in tables II to IV and are plotted in dimensionless form as a function of tip-speed ratio in figure 13. Separate plots are presented for each collective pitch angle. The data points presented are

for three different values of gust velocity and for the three different values of flapping hinge offset. The differences between the flapping coefficients associated with these nine test conditions are of a random nature and are generally within the range of the scatter in the data. No distinction is made in the data points presented for the different gust velocities; however, the different values of flapping hinge offset are designated. The results presented in figure 13 show that the flapping coefficient is essentially independent of both gust velocity and flapping hinge offset.

Figure 13 shows that, at a given value of μ, $B_{\Delta\bar{\beta}}$ generally increases with collective pitch angle. At a pitch angle of 6.6°, the variation in $B_{\Delta\bar{\beta}}$ with μ is very similar to that exhibited by the thrust coefficient in figure 10 and indicates that $B_{\Delta\bar{\beta}}$ is reduced by the effects of blade stall.

The fact that $B_{\Delta\bar{\beta}}$ is dependent on θ indicates that the response of the rotor due to interception of a sharp-edge gust is dependent on the conditions of rotor inflow prior to entering the gust.

A calculation of the flapping response of a blade with $\gamma = 12$ (a lighter blade than that of the present tests where the average value of $\gamma \approx 7$) was made in reference 6 for the blade intercepting a sharp-edge gust at $\mu = 0.2$. The corresponding value of $B_{\Delta\bar{\beta}}$ obtained was 188 which is approximately equal to the value obtained in the present tests for $\theta = 6.6^{\circ}$. The theoretical analysis assumes that the incremental changes in $B_{\Delta\bar{\beta}}$ are independent of the initial conditions and thus independent of θ and the associated effects of stall. The experimental results show, however, that such is not the case.

Blade Bending Moments

Figure 14 presents typical plots showing the variations in the blade spanwise bending-moment distribution with tip-speed ratio for all test configurations at one gust velocity and one collective pitch angle. These variations were obtained by normalizing the data on the maximum bending-moment coefficient calculated for these test conditions ($B_{\Delta M} = 0.132$ at $\mu = 0.15$ and $r/R = 0.25$ for the fixed-at-root configuration). These plots show the reductions in bending moments achieved by the use of flapping hinges. They also show that, when flapping hinges are used, the bending moments due to gust disturbances can be reduced by increasing the amount of flapping hinge offset. Figure 14 further shows that the bending moment measured at the most inboard station is the maximum in all cases. In addition, it appears that in some cases the bending moment at $r/R = 0.42$ is less than the corresponding moments at $r/R = 0.625$. This

is apparently due to the fact that a significant portion of the blade moments results from bending in the second elastic mode which, due to the characteristic curvature of this mode, exhibits very little moment in the vicinity of $r/R = 0.42$. (See fig. 3 of ref. 12.)

As shown in figure 14 and as indicated in the tables, the highest bending moments were measured at $r/R = 0.25$. Figures 15 and 16 present a summary of the values of $B_{\Delta M}$ measured at $r/R = 0.25$ for the various test conditions for the fixed-at-root and flapping rotors, respectively.

The variation of $B_{\Delta M}$ with μ shown in figure 15 for the fixed-at-root configuration for the different values of θ exhibits trends very similar to those observed for $B_{\Delta\bar{\beta}}$ in figure 13 and shows that the increment in blade bending moment produced by a sharp-edge gust is dependent on the rotor inflow prior to gust entry. Data are presented for the three gust velocities but the differences in $B_{\Delta M}$ were found to be within the scatter of the data and therefore no differentiation in gust velocity is made. A mean value for $B_{\Delta M}$ of 0.08 seems to be representative of the data obtained at $r/R = 0.25$.

The data presented in figure 16 show that $B_{\Delta M}$ at $r/R = 0.25$ for the flapping configurations, in contrast to the fixed-at-root configuration, tends to decrease somewhat at the higher test values of μ as the collective pitch angle increases. The differences in the data for the different gust velocities are again within the range of scatter and no distinction between gust velocities is made. The data do indicate, however, that the bending moments at low values of μ decrease somewhat as the flapping hinge offset is increased. Values for $B_{\Delta M}$ of 0.01 to 0.035 seem to be representative for $r/R = 0.25$, the lower values corresponding to the higher values of flapping hinge offset. Some of this reduction in bending moment at $r/R = 0.25$ due to increase in flapping hinge offset may be due to a shift of the spanwise location of the bending gage relative to the spanwise location of the maximum moment as the amount of flapping hinge offset is increased.

The results of the analytical study of reference 6 indicate that most of the bending moments which arise when a hinged rotor blade penetrates a sharp-edge gust are associated with bending in the higher modes. The results of the present study also indicate this to be true as evidenced by the high-frequency components of the bending moments. (For example, see fig. 10.) Among the parameters which influence the blade bending response is the ratio of the rotor speed to the various natural frequencies of the nonrotating blade $\left(\text{that is, } \frac{\Omega^2 mR^4}{EI}\right)$. A comparison of the values of this parameter shows that the value used for the calculations in reference 6 is approximately twice the value for the blades

tested during this investigation. However, in order to get some idea of the comparative values of $B_{\Delta M}$ for the two studies, the maximum values obtained at a tip-speed ratio of 0.2 were calculated and the results of reference 6 yield a value of $B_{\Delta M} = 0.021$ which is approximately equal to values given in figure 16. It should be noted, however, that the results of reference 6 indicate this value to be at $r/R = 0.45$, whereas the maximum moment on the blades tested in this investigation occurred at $r/R = 0.25$.

SUMMARY OF RESULTS

The results of this experimental investigation of the incremental changes in the periodic components of the flapping angle and bending-moment responses of rotor blades due to penetration of a sharp-edge gust may be summarized as follows:

1. The dimensionless flapping coefficient $B_{\Delta\bar{\beta}}$ derived by the application of the principles of dimensional analysis is found to be essentially independent of both gust velocity and flapping hinge offset. This coefficient varies considerably with tip-speed ratio, generally increases with collective pitch angle, and is reduced by the effects of blade stall. The results are in substantial agreement with available theory at collective pitch angles approximately equal to those encountered under usual conditions of flight but show that the assumption of independence of response and collective pitch angle is inadequate.

2. A dimensionless coefficient was also derived for the blade bending response $B_{\Delta M}$ and the results show that this coefficient is also essentially independent of gust velocity but dependent on both tip-speed ratio and collective pitch angle. For the fixed-at-root blade, a mean value of $B_{\Delta M}$ of 0.08 at one-fourth of the blade radius appears to be representative, whereas, for blades having flapping hinges, the value of $B_{\Delta M}$ at the same blade station is reduced to 0.01 to 0.035, the lower values being associated with higher values of flapping hinge offset. Again the results are in fair agreement with theory, but at variance with the theoretical assumptions of independence of collective pitch angle.

Langley Research Center,
National Aeronautics and Space Administration,
Langley Field, Va., April 27, 1959.

APPENDIX

DERIVATION OF DIMENSIONLESS COEFFICIENTS FOR ROTOR-BLADE BENDING-MOMENT AND FLAPPING-ANGLE RESPONSES DURING PENETRATION OF SHARP-EDGE GUSTS

This appendix presents the derivation, on the basis of dimensional analysis, of dimensionless parameters which are used to present the data obtained during the present investigation and to correlate the results of this study with other studies of a similar nature. The derivation consists of listing the important variables of the problem and grouping these in such a fashion as to obtain appropriate dimensionless parameters for both blade bending moments and flapping angles. This approach is conventional and is presented here because its application to this problem may be of some specific interest.

Let the periodic components of the blade flapping angle and blade bending moments at a given spanwise station which arise as a result of rotor penetration of a sharp-edge gust be $\Delta\bar{\beta}$ and ΔM, respectively. Then $\Delta\bar{\beta}$ and ΔM are given by the following relationships:

$$\Delta\bar{\beta} = A\left(\rho^{a_1} U^{a_2} V^{a_3} \Omega^{a_4} R^{a_5} c^{a_6} r^{a_7} e^{a_8} m^{a_9} I^{a_{10}}\right) \tag{A1}$$

$$\Delta M = B\left(\rho^{b_1} U^{b_2} V^{b_3} \Omega^{b_4} R^{b_5} c^{b_6} r^{b_7} e^{b_8} m^{b_9} (EI)^{b_{10}}\right) \tag{A2}$$

where

$a_1, a_2, \ldots a_{10}$
$b_1, b_2, \ldots b_{10}$ } undetermined constant exponents

A,B constants

ρ air density

U gust velocity

V forward velocity of rotor

Ω rotor speed

R rotor radius

c	blade chord
r	radial location of gust front along blade
e	blade flapping hinge offset
m	mass per unit length of the blade
I	mass moment of inertia of the blade about the flapping hinge
EI	flapwise flexural rigidity of the blade

Now let M, L, and T be representative units of mass, length, and time, and the dimensional forms of equations (A1) and (A2) are

$$0 = \left(\frac{M}{L^3}\right)^{a_1}\left(\frac{L}{T}\right)^{a_2}\left(\frac{L}{T}\right)^{a_3}\left(\frac{1}{T}\right)^{a_4}(L)^{a_5}(L)^{a_6}(L)^{a_7}(L)^{a_8}\left(\frac{M}{L}\right)^{a_9}(ML^2)^{a_{10}} \quad . \quad . \quad . \quad (A3)$$

$$\frac{ML^2}{T^2} = \left(\frac{M}{L^3}\right)^{b_1}\left(\frac{L}{T}\right)^{b_2}\left(\frac{L}{T}\right)^{b_3}\left(\frac{1}{T}\right)^{b_4}(L)^{b_5}(L)^{b_6}(L)^{b_7}(L)^{b_8}\left(\frac{M}{L}\right)^{b_9}\left(\frac{ML^3}{T^2}\right)^{b_{10}} \quad . \quad . \quad . \quad (A4)$$

The equation of exponents of M, L, and T for each side of equations (A3) and (A4) yields three equations for the determination of each set of exponents. This relationship means that the most information that one can gain from dimensional analysis is a reduction of the number of exponents by three in each case by expressing three of the a exponents in terms of the remaining a exponents and three of the b exponents in terms of the remaining b exponents. This procedure, however, leads to a rearrangement of the variables in many possible dimensionless forms depending on which exponents are eliminated. The resulting dimensionless forms which seem most logical are derived by the elimination of a_4, a_5, and a_{10} in equation (A3) and b_4, b_5, and b_{10} in equation (A4). With these choices, equations (A1) and (A2) reduce to

$$\Delta\bar{\beta} = A\left[\left(\frac{\rho R^5}{I}\right)^{a_1}\left(\frac{U}{\Omega R}\right)^{a_2}\left(\frac{V}{\Omega R}\right)^{a_3}\left(\frac{c}{R}\right)^{a_6}\left(\frac{r}{R}\right)^{a_7}\left(\frac{e}{R}\right)^{a_8}\left(\frac{mR^3}{I}\right)^{a_9}\right] \quad . \quad . \quad . \quad (A5)$$

$$\frac{\Delta M}{EI/R} = B\left[\left(\frac{\rho R^6\Omega^2}{EI}\right)^{b_1}\left(\frac{U}{\Omega R}\right)^{b_2}\left(\frac{V}{\Omega R}\right)^{b_3}\left(\frac{c}{R}\right)^{b_6}\left(\frac{r}{R}\right)^{b_7}\left(\frac{e}{R}\right)^{b_8}\left(\frac{m\Omega^2R^4}{EI}\right)^{b_9}\right] \quad . \quad . \quad . \quad (A6)$$

Equations (A5) and (A6) show that a considerable number of dimensionless coefficients are involved. Actually, there are other factors

which, themselves, appear in dimensionless form which have not yet been considered but must be included. These are the various rotor angles, namely,

α rotor angle of attack

θ rotor collective pitch angle

ψ_g azimuth angle at which a designated blade intercepts the gust front.

The Reynolds number N_{Re} and slope of the lift curve a may also be important and may be added as the dimensionless coefficients.

It is well known that other dimensionless parameters may be obtained by multiplication or division of those obtained by the elimination of any given set of the exponents a_1, a_2, and so forth. In the present case, some variations of the forms presented in equations (A5) and (A6) are desirable.

In the case of flapping, it is desirable to reduce the factor $\frac{\rho R^5}{I}$ to the conventional helicopter parameter γ and to eliminate the inertia term from the factor $\frac{mR^3}{I}$. Equation (A5) may be put in the functional form

$$\Delta\bar{\beta} = f\left(\gamma, \frac{U}{\Omega R}, \mu, \frac{c}{R}, \frac{r}{R}, \frac{e}{R}, \frac{\rho c^2}{m}, \alpha, \theta, \psi_g, a, N_{Re}\right) \ldots \qquad (A7)$$

where

μ tip-speed ratio $= \frac{V}{\Omega R}$

γ Lock number $= \frac{cR^4 a\rho}{I} = \frac{\rho R^5}{I} a \frac{c}{R}$

a slope of lift curve

$$\frac{\rho c^2}{m} = \frac{\gamma I}{mR^3} \frac{1}{a} \frac{c}{R}$$

Since the quantity $\frac{U}{\Omega R}$ is an effective angle of attack of the blade tip element, it seems logical that $\Delta\bar{\beta}$ should be, to the first order of

approximation, proportional to $\frac{U}{\Omega R}$. With this assumption, a dimensionless parameter for $\Delta\bar{\beta}$ is suggested which involves the ratio of $\Delta\bar{\beta}$ to $\frac{U}{\Omega R}$.

$$B_{\Delta\bar{\beta}} = \frac{\Delta\bar{\beta}}{\frac{U}{\Omega R}} = f_1\left(\gamma, \frac{U}{\Omega R}, \mu, \frac{c}{R}, \frac{r}{R}, \frac{e}{R}, \frac{\rho c^2}{m}, \alpha, \theta, \psi_g, a, N_{Re}\right) \quad . \quad . \quad . \qquad (A8)$$

and two rotors having similar values of all the parameters within the brackets of equation (A8) should yield similar flapping responses $B_{\Delta\bar{\beta}}$. It should be noted that changes in inertia effects due to flapping hinge offset are partially contained in γ due to its dependence on the moment of inertia about the flapping hinge.

In the case of rotor-blade bending, some rearrangement of the dimensionless parameters in equation (A6) is desirable. For example, the ratio $\frac{\Omega^2}{EI}$ which appears in two terms can be treated in a single term by the following arrangement:

$$\frac{\rho R^6 \Omega^2}{EI} = \frac{\rho c^2}{m} \frac{m R^4 \Omega^2}{EI} \left(\frac{R}{c}\right)^2$$

The functional form of equation (A6) then reduces to

$$\frac{\Delta M}{EI/R} = g\left(\frac{\rho c^2}{m}, \frac{U}{\Omega R}, \mu, \frac{c}{R}, \frac{r}{R}, \frac{e}{R}, \frac{m\Omega^2 R^4}{EI}, \alpha, \theta, \psi_g, a, N_{Re}\right) \quad . \quad . \quad . \qquad (A9)$$

Physically, ΔM is not expected to be proportional to EI; however, it is expected to have a first-order linear dependence on both the density and the gust velocity. This requirement suggests the formation of a bending-moment coefficient involving the ratio of $\frac{\Delta M}{EI/R}$ to the product $\frac{\rho R c}{m} \frac{U}{\Omega R} \frac{m\Omega^2 R^4}{EI}$, that is,

$$B_{\Delta M} = \frac{\Delta M}{\rho U (\Omega R) c R^2} = g_1\left(\frac{\rho R c}{m}, \frac{U}{\Omega R}, \mu, \frac{c}{R}, \frac{e}{R}, \frac{m\Omega^2 R^4}{EI}, \alpha, \theta, \psi_g, a, N_{Re}\right) \quad . \quad . \quad . \qquad (A10)$$

and two rotors having similar values of all parameters within the parentheses of equation (A10) would be expected to exhibit similar blade bending-moment responses $B_{\Delta M}$.

The factor $\frac{\Omega^2 mR^4}{EI}$ may be interpreted as a function of $\frac{\Omega^2}{\omega_n^2}$ where ω_n is the natural bending frequency of the nth mode of the nonrotating blade.

REFERENCES

1. Gustafson, F. B., and Crim, Almer D.: Flight Measurements and Analysis of Helicopter Normal Load Factors in Maneuvers. NACA TN 2990, 1953.

2. Crim, Almer D.: Gust Experience of a Helicopter and an Airplane in Formation Flight. NACA TN 3354, 1954.

3. Ludi, LeRoy H.: Flight Investigation of Effects of Atmospheric Turbulence and Moderate Maneuvers on Bending and Torsional Moments Encountered by a Helicopter Rotor Blade. NACA TN 4203, 1958.

4. Jewel, Joseph W., Jr., and Carpenter, Paul J.: A Preliminary Investigation of the Effects of Gusty Air on Helicopter-Blade Bending Moments. NACA TN 3074, 1954.

5. Maglieri, Domenic J., and Reisert, Thomas D.: Gust-Tunnel Investigation of the Effect of a Sharp-Edge Gust on the Flapwise Blade Bending Moments of a Model Helicopter Rotor. NACA TN 3470, 1955.

6. Michel, D., Polleys, E., Berman, A., Shulman, Y., and Nagem, M.: Dynamic Response of a Helicopter to a Gust. Rep. No. R-30 (Contract NOa(s) 53-318c), The Kaman Aircraft Corp.
   Pt. I. Feb. 28, 1957.
   Pt. II. Feb. 28, 1957.
   Pt. III. Feb. 28, 1957.
   Pt. IV. Jan. 31, 1958.

7. Yntema, Robert T.: Simplified Procedures and Charts for the Rapid Estimation of Bending Frequencies of Rotating Beams. NACA TN 3459, 1955. (Supersedes NACA RM L54G02.)

8. Donely, Philip: Summary of Information Relating to Gust Loads on Airplanes. NACA Rep. 997, 1950. (Supersedes NACA TN 1976.)

9. Jacobs, Eastman N., and Sherman, Albert: Airfoil Section Characteristics As Affected by Variations of the Reynolds Number. NACA Rep. 586, 1937.

10. Gessow, Alfred, and Myers, Garry C., Jr.: Aerodynamics of the Helicopter. The MacMillan Co., c.1952.

11. McCarty, John Locke, Brooks, George W., and Maglieri, Domenic J.: Wind-Tunnel Investigation of the Effect of Angle of Attack and Flapping-Hinge Offset on Periodic Bending Moments and Flapping of a Small Rotor. NASA MEMO 3-3-59L, 1959.

12. Daughaday, H., and Kline, J.: An Approach to the Determination of Higher Harmonic Rotor Blade Stresses. Proc. Ninth Annual Forum, Am. Helicopter Soc., Inc., May 14-17, 1953, pp. 90-126.

TABLE I.- TABULATION OF BLADE BENDING-MOMENT DATA FOR FIXED-AT-ROOT CONFIGURATION

$\theta = 0.6^\circ$

μ	$\bar{\beta}$	$\Delta\bar{\beta}$	$\frac{r}{R} = 0.25$ M	$\frac{r}{R} = 0.25$ ΔM	$\frac{r}{R} = 0.42$ M	$\frac{r}{R} = 0.42$ ΔM	$\frac{r}{R} = 0.625$ M	$\frac{r}{R} = 0.625$ ΔM	$\frac{r}{R} = 0.833$ M	$\frac{r}{R} = 0.833$ ΔM
U = 5 ft/sec										
0.02	---	---	1.20	1.06	0.21	0.17	0.12	0.06	0.11	0.05
.03	---	---	1.19	1.02	.21	.17	.13	.07	.11	.04
.045	---	---	1.16	.96	.20	.16	.14	.08	.12	.05
.06	---	---	1.14	.92	.20	.15	.16	.09	.12	.05
.075	---	---	1.11	.87	.20	.15	.16	.09	.13	.06
.09	---	---	1.08	.81	.20	.15	.17	.11	.13	.06
.12	---	---	1.02	.71	.21	.15	.18	.12	.12	.05
.15	---	---	.98	.61	.21	.14	.18	.11	.12	.04
.18	---	---	.95	.53	.22	.13	.19	.10	.12	.03
.24	---	---	1.20	.63	.29	.15	.26	.12	.14	.01
U = 7.5 ft/sec										
0.02	---	---	1.85	1.71	0.30	0.26	0.21	0.15	0.13	0.07
.03	---	---	1.80	1.63	.30	.26	.22	.16	.15	.08
.045	---	---	1.71	1.51	.30	.26	.24	.18	.16	.09
.06	---	---	1.64	1.42	.31	.26	.25	.18	.18	.11
.075	---	---	1.58	1.34	.32	.27	.26	.19	.18	.11
.09	---	---	1.54	1.27	.32	.27	.26	.20	.18	.11
.12	---	---	1.50	1.19	.33	.27	.26	.20	.18	.11
.15	---	---	1.48	1.11	.34	.27	.26	.19	.17	.09
.18	---	---	1.53	1.11	.34	.25	.26	.17	.16	.07
.24	---	---	1.86	1.29	.36	.22	.28	.14	.16	.03
U = 10 ft/sec										
0.02	---	---	2.65	2.51	0.44	0.40	0.27	0.21	0.23	0.17
.03	---	---	2.57	2.40	.44	.40	.31	.25	.22	.15
.045	---	---	2.44	2.24	.44	.40	.33	.27	.22	.15
.06	---	---	2.33	2.11	.44	.39	.33	.26	.21	.14
.075	---	---	2.24	2.00	.44	.39	.33	.26	.21	.14
.09	---	---	2.18	1.91	.44	.39	.33	.27	.20	.13
.12	---	---	2.11	1.80	.44	.38	.33	.27	.20	.13
.15	---	---	2.18	1.81	.45	.38	.33	.26	.20	.12
.18	---	---	2.34	1.92	.47	.38	.34	.25	.20	.11
.24	---	---	2.79	2.22	.56	.42	.36	.22	.22	.09

$\theta = 3.4^\circ$

μ	$\bar{\beta}$	$\Delta\bar{\beta}$	$\frac{r}{R} = 0.25$ M	$\frac{r}{R} = 0.25$ ΔM	$\frac{r}{R} = 0.42$ M	$\frac{r}{R} = 0.42$ ΔM	$\frac{r}{R} = 0.625$ M	$\frac{r}{R} = 0.625$ ΔM	$\frac{r}{R} = 0.833$ M	$\frac{r}{R} = 0.833$ ΔM
U = 5 ft/sec										
0.02	---	---	1.51	0.92	0.35	0.19	0.34	0.16	0.25	0.09
.03	---	---	1.68	.98	.38	.19	.35	.14	.26	.07
.045	---	---	1.79	.96	.41	.20	.36	.10	.26	.04
.06	---	---	1.88	.96	.44	.21	.36	.08	.25	.03
.075	---	---	1.96	.96	.45	.22	.36	.07	.24	.01
.09	---	---	2.05	.96	.45	.20	.36	.06	.23	.01
.12	---	---	2.26	.98	.48	.23	.34	.06	.22	.02
.15	---	---	2.63	1.07	.52	.22	.32	.07	.21	.03
.18	---	---	3.21	1.06	.58	.21	.35	.07	.22	.03
.24	---	---	4.27	1.65	.87	.38	.47	.05	.30	.04
U = 7.5 ft/sec										
0.02	---	---	1.96	1.37	0.39	0.23	0.37	0.19	0.29	0.13
.03	---	---	2.15	1.45	.44	.25	.38	.17	.29	.10
.045	---	---	2.26	1.43	.48	.27	.38	.12	.27	.05
.06	---	---	2.32	1.40	.50	.27	.38	.10	.26	.04
.075	---	---	2.39	1.39	.52	.29	.37	.08	.24	.01
.09	---	---	2.49	1.40	.52	.27	.38	.08	.24	.02
.12	---	---	2.99	1.71	.58	.33	.42	.14	.30	.10
.15	---	---	3.62	2.06	.71	.41	.48	.23	.37	.19
.18	---	---	4.21	2.06	.82	.45	.55	.27	.42	.23
.24	---	---	5.30	2.68	.95	.46	.65	.23	.40	.20
U = 10 ft/sec										
0.02	---	---	2.49	1.90	0.49	0.33	0.36	0.18	0.26	0.10
.03	---	---	2.61	1.91	.52	.33	.38	.17	.28	.09
.045	---	---	2.73	1.90	.55	.34	.40	.14	.28	.06
.06	---	---	2.83	1.91	.57	.34	.40	.12	.28	.06
.075	---	---	3.00	2.00	.59	.36	.40	.11	.28	.05
.09	---	---	3.27	2.18	.62	.37	.41	.11	.30	.08
.12	---	---	3.82	2.54	.74	.39	.48	.20	.39	.19
.15	---	---	4.49	2.93	.85	.55	.60	.35	.44	.26
.18	---	---	5.28	3.13	.94	.57	.72	.44	.48	.29
.24	---	---	----	----	----	----	----	----	----	----

$\theta = 6.6^\circ$

μ	$\bar{\beta}$	$\Delta\bar{\beta}$	$\frac{r}{R} = 0.25$ M	$\frac{r}{R} = 0.25$ ΔM	$\frac{r}{R} = 0.42$ M	$\frac{r}{R} = 0.42$ ΔM	$\frac{r}{R} = 0.625$ M	$\frac{r}{R} = 0.625$ ΔM	$\frac{r}{R} = 0.833$ M	$\frac{r}{R} = 0.833$ ΔM
U = 5 ft/sec										
0.02	---	---	1.53	0.69	0.35	0.13	0.33	0.13	0.27	0.11
.03	---	---	1.87	.84	.42	.15	.38	.14	.29	.12
.045	---	---	2.18	.85	.50	.17	.43	.13	.31	.11
.06	---	---	2.46	.87	.55	.19	.44	.11	.32	.08
.075	---	---	2.73	.90	.59	.20	.46	.10	.34	.06
.09	---	---	3.09	.97	.67	.24	.48	.11	.36	.05
.12	---	---	3.96	1.28	.83	.31	.52	.12	.39	.02
.15	---	---	4.91	1.60	1.01	.39	.58	.18	.42	.07
.18	---	---	5.94	1.93	1.13	.36	.66	.20	.46	.10
.24	---	---	7.09	1.54	1.28	.20	.91	.18	.62	.21
U = 7.5 ft/sec										
0.02	---	---	1.69	0.85	0.40	0.18	0.34	0.14	0.24	0.08
.03	---	---	2.04	1.01	.48	.21	.39	.15	.26	.09
.045	---	---	2.36	1.03	.57	.24	.46	.16	.29	.09
.06	---	---	3.08	1.49	.65	.29	.51	.18	.32	.08
.075	---	---	3.55	1.72	.73	.34	.55	.19	.35	.07
.09	---	---	4.01	1.89	.83	.40	.59	.22	.38	.07
.12	---	---	4.81	2.13	1.00	.48	.65	.25	.44	.07
.15	---	---	5.52	2.21	1.14	.52	.72	.29	.49	.14
.18	---	---	6.21	2.20	1.25	.48	.80	.34	.55	.19
.24	---	---	7.55	2.00	1.34	.26	1.05	.42	.74	.33
U = 10 ft/sec										
0.02	---	---	2.65	1.81	0.46	0.24	0.40	0.20	0.26	0.10
.03	---	---	3.19	2.16	.56	.29	.49	.25	.32	.15
.045	---	---	3.75	2.42	.69	.36	.59	.29	.38	.18
.06	---	---	4.13	2.54	.79	.43	.64	.31	.40	.16
.075	---	---	4.47	2.54	.87	.48	.66	.30	.43	.15
.09	---	---	4.82	2.70	.95	.52	.67	.30	.44	.13
.12	---	---	5.52	2.84	1.09	.57	.69	.29	.50	.13
.15	---	---	6.19	2.88	1.21	.59	.77	.34	.56	.21
.18	---	---	6.83	2.82	1.31	.54	.89	.43	.62	.26
.24	---	---	7.98	2.43	1.53	.45	1.20	.57	.72	.31

TABLE II.- TABULATION OF BLADE FLAPPING AND BENDING-MOMENT DATA FOR FLAPPING CONFIGURATION (e/R = 0)

$\theta = 0.6^\circ$

μ	$\bar{\beta}$	$\Delta\bar{\beta}$	$\frac{r}{R} = 0.25$ M	$\frac{r}{R} = 0.25$ ΔM	$\frac{r}{R} = 0.42$ M	$\frac{r}{R} = 0.42$ ΔM	$\frac{r}{R} = 0.625$ M	$\frac{r}{R} = 0.625$ ΔM	$\frac{r}{R} = 0.833$ M	$\frac{r}{R} = 0.833$ ΔM
U = 5 ft/sec										
0.02	3.20	2.85	0.31	0.20	0.12	0.06	0.12	0.06	0.09	0.03
.03	3.00	2.55	.35	.23	.15	.09	.15	.09	.11	.05
.045	2.80	2.40	.43	.30	.18	.12	.17	.10	.13	.07
.06	2.70	2.40	.46	.32	.19	.12	.18	.11	.13	.08
.075	2.65	2.25	.47	.32	.19	.12	.17	.10	.13	.09
.09	2.60	2.10	.48	.32	.19	.11	.17	.10	.12	.08
.12	2.55	1.85	.48	.30	.19	.10	.17	.10	.11	.06
.15	2.50	1.70	.46	.26	.19	.10	.16	.08	.11	.03
.18	2.55	1.55	.44	.18	.19	.07	.16	.06	.12	.03
.24	3.25	2.10	.39	.03	.19	.07	.16	.02	.14	.03
U = 7.5 ft/sec										
0.02	4.45	4.05	0.40	0.29	0.18	0.12	0.16	0.10	0.14	0.08
.03	4.20	3.80	.52	.40	.21	.15	.18	.12	.15	.09
.045	3.95	3.55	.59	.46	.23	.17	.20	.13	.15	.09
.06	3.85	3.45	.61	.47	.24	.17	.21	.14	.14	.09
.075	3.80	3.40	.60	.45	.24	.17	.21	.14	.12	.08
.09	3.75	3.25	.57	.41	.24	.16	.21	.14	.12	.08
.12	3.70	3.10	.54	.36	.24	.15	.20	.13	.13	.08
.15	3.70	2.90	.57	.37	.24	.15	.21	.13	.15	.07
.18	3.60	2.70	.61	.35	.23	.11	.23	.13	.16	.07
.24	5.20	4.00	.68	.32	.21	.04	.29	.15	.17	.06
U = 10 ft/sec										
0.02	6.45	6.05	0.79	0.68	0.33	0.27	0.24	0.18	0.19	0.13
.03	5.75	5.35	.77	.65	.31	.25	.26	.20	.20	.14
.045	5.25	4.85	.76	.63	.29	.23	.29	.22	.21	.15
.06	5.05	4.65	.75	.61	.28	.21	.31	.24	.22	.17
.075	4.93	4.53	.75	.60	.28	.21	.32	.25	.23	.19
.09	4.90	4.40	.75	.59	.28	.20	.32	.25	.23	.19
.12	4.95	4.35	.75	.57	.29	.20	.32	.25	.21	.16
.15	5.15	4.35	.75	.55	.30	.21	.29	.21	.18	.10
.18	5.45	4.55	.78	.52	.34	.22	.28	.18	.19	.10
.24	7.50	6.30	.91	.55	.45	.28	.41	.27	.29	.18

$\theta = 3.4^\circ$

μ	$\bar{\beta}$	$\Delta\bar{\beta}$	$\frac{r}{R} = 0.25$ M	$\frac{r}{R} = 0.25$ ΔM	$\frac{r}{R} = 0.42$ M	$\frac{r}{R} = 0.42$ ΔM	$\frac{r}{R} = 0.625$ M	$\frac{r}{R} = 0.625$ ΔM	$\frac{r}{R} = 0.833$ M	$\frac{r}{R} = 0.833$ ΔM
U = 5 ft/sec										
0.02	2.90	1.40	0.48	0.35	0.20	0.12	0.26	0.14	0.19	0.07
.03	3.50	1.45	.59	.40	.24	.13	.27	.12	.20	.07
.045	3.50	1.35	.66	.38	.27	.12	.29	.11	.19	.05
.06	3.53	1.13	.68	.31	.29	.11	.29	.10	.17	.03
.075	3.65	1.25	.66	.23	.28	.08	.28	.08	.14	0
.09	3.80	1.40	.64	.18	.28	.07	.26	.06	.12	-.01
.12	4.30	2.10	.60	.14	.26	.05	.21	.02	.13	.01
.15	5.16	2.60	.59	.14	.25	.04	.22	.05	.18	.03
.18	6.04	3.05	.64	.12	.26	.04	.30	.10	.26	.10
.24	7.20	3.50	.80	.18	.30	.09	.36	.14	.28	.08
U = 7.5 ft/sec										
0.02	3.35	1.85	0.46	0.33	0.23	0.15	0.22	0.10	0.25	0.13
.03	3.90	2.00	.56	.37	.24	.13	.20	.05	.22	.09
.045	4.18	1.98	.65	.37	.27	.12	.22	.04	.20	.06
.06	4.10	1.70	.70	.33	.30	.12	.25	.06	.20	.06
.075	4.13	1.73	.72	.29	.31	.11	.26	.06	.20	.06
.09	4.38	1.98	.72	.26	.31	.10	.27	.07	.21	.08
.12	5.44	3.24	.70	.24	.31	.10	.29	.10	.25	.13
.15	6.90	4.40	.69	.24	.31	.10	.34	.17	.29	.14
.18	7.85	4.85	.71	.19	.31	.09	.39	.19	.34	.18
.24	8.85	5.15	.69	.07	.31	.10	.42	.20	.32	.12
U = 10 ft/sec										
0.02	3.87	2.37	0.41	0.28	0.21	0.13	0.20	0.08	0.21	0.09
.03	4.35	2.45	.58	.39	.24	.13	.23	.08	.22	.09
.045	4.75	2.55	.70	.42	.32	.17	.26	.08	.23	.09
.06	4.85	2.45	.76	.39	.34	.16	.30	.11	.25	.11
.075	4.80	2.40	.80	.37	.35	.15	.33	.13	.26	.12
.09	4.95	2.55	.81	.35	.35	.14	.35	.15	.28	.15
.12	7.00	4.80	.80	.34	.35	.14	.39	.20	.30	.18
.15	8.30	5.80	.77	.32	.35	.14	.40	.23	.31	16
.18	8.85	5.85	.76	.24	.35	.13	.40	.20	.32	.16
.24	9.30	5.60	.92	.30	.37	.16	.44	.22	.29	.09

$\theta = 6.6^\circ$

μ	$\bar{\beta}$	$\Delta\bar{\beta}$	$\frac{r}{R} = 0.25$ M	$\frac{r}{R} = 0.25$ ΔM	$\frac{r}{R} = 0.42$ M	$\frac{r}{R} = 0.42$ ΔM	$\frac{r}{R} = 0.625$ M	$\frac{r}{R} = 0.625$ ΔM	$\frac{r}{R} = 0.833$ M	$\frac{r}{R} = 0.833$ ΔM
U = 5 ft/sec										
0.02	4.30	2.10	0.71	0.45	0.26	0.15	0.32	0.15	0.27	0.11
.03	5.20	2.20	.78	.46	.29	.16	.33	.13	.29	.11
.045	5.80	2.00	.81	.43	.29	.12	.35	.13	.31	.11
.06	6.50	2.10	.78	.35	.26	.06	.36	.12	.31	.11
.075	7.30	2.20	.75	.28	.26	.03	.36	.11	.29	.09
.09	8.60	2.90	.75	.24	.28	.03	.36	.09	.29	.10
.12	12.00	4.95	.79	.21	.30	.05	.35	.05	.31	.08
.15	14.20	5.45	.83	.18	.30	.05	.35	.02	.33	.02
.18	15.45	4.65	.87	.17	.30	.05	.35	-.01	.35	.01
.24	17.30	4.10	.85	.09	.31	.03	.36	-.05	.33	-.02
U = 7.5 ft/sec										
0.02	5.10	2.90	0.58	0.32	0.28	0.17	0.31	0.14	0.24	0.08
.03	6.00	3.00	.63	.31	.26	.13	.28	.08	.26	.08
.045	7.50	3.70	.69	.31	.27	.10	.29	.07	.31	.11
.06	8.90	4.50	.73	.30	.29	.09	.31	.07	.33	.13
.075	10.30	5.25	.75	.28	.31	.08	.33	.08	.30	.10
.09	11.65	5.95	.78	.27	.33	.08	.35	.08	.29	.10
.12	14.00	6.95	.85	.27	.38	.13	.39	.09	.33	.10
.15	15.80	7.05	.94	.29	.42	.17	.43	.10	.37	.06
.18	17.20	6.40	.98	.28	.44	.19	.43	.07	.37	.03
.24	19.70	6.50	.96	.20	.39	.11	.44	.03	.41	.06
U = 10 ft/sec										
0.02	6.50	4.30	0.59	0.33	0.22	0.11	0.23	0.06	0.22	0.06
.03	7.90	4.90	.68	.36	.26	.13	.27	.07	.25	.07
.045	9.80	6.00	.76	.38	.31	.14	.33	.11	.29	.09
.06	11.40	7.00	.83	.40	.35	.15	.37	.13	.32	.12
.075	12.70	7.65	.88	.41	.38	.15	.42	.17	.34	.14
.09	13.80	8.10	.91	.40	.40	.15	.44	.17	.36	.17
.12	15.55	8.50	.88	.30	.38	.13	.42	.12	.35	.12
.15	17.00	8.25	.91	.26	.37	.12	.42	.09	.38	.07
.18	18.40	7.60	.96	.26	.39	.14	.46	.10	.43	.09
.24	20.90	7.70	.94	.18	.45	.17	.49	.08	.50	.15

TABLE III.- TABULATION OF BLADE FLAPPING AND BENDING-MOMENT DATA FOR FLAPPING CONFIGURATION (e/R = 0.05)

μ	θ = 0.6°									
	$\bar{\beta}$	$\Delta\bar{\beta}$	$\frac{r}{R}$ = 0.25		$\frac{r}{R}$ = 0.42		$\frac{r}{R}$ = 0.625		$\frac{r}{R}$ = 0.833	
			M	ΔM	M	ΔM	M	ΔM	M	ΔM
U = 5 ft/sec										
0.02	4.00	3.00	0.27	0.16	0.12	0.06	0.12	0.06	0.11	0.05
.03	3.80	2.80	.31	.21	.14	.09	.14	.08	.11	.05
.045	3.45	2.40	.35	.26	.16	.12	.15	.10	.10	.05
.06	3.20	2.10	.37	.28	.17	.13	.15	.10	.10	.05
.075	3.15	2.00	.37	.28	.17	.13	.14	.09	.11	.07
.09	3.10	1.90	.37	.28	.16	.12	.13	.08	.11	.08
.12	3.05	1.85	.38	.28	.16	.11	.14	.08	.12	.08
.15	3.00	1.70	.39	.29	.17	.11	.16	.09	.13	.06
.18	3.05	1.45	.40	.28	.19	.10	.19	.12	.14	.06
.24	4.00	1.45	.46	.20	.23	.08	.21	.10	.16	.08
U = 7.5 ft/sec										
0.02	6.45	5.45	0.41	0.30	0.17	0.11	0.16	0.10	0.13	0.07
.03	5.84	4.85	.43	.33	.18	.13	.17	.11	.14	.08
.045	5.30	4.25	.46	.37	.19	.15	.19	.14	.15	.10
.06	5.00	3.90	.49	.40	.21	.17	.20	.15	.15	.10
.075	4.85	3.70	.50	.41	.22	.18	.20	.15	.14	.10
.09	4.85	3.65	.50	.41	.22	.18	.21	.16	.14	.11
.12	4.72	3.52	.48	.38	.22	.17	.21	.15	.15	.11
.15	4.42	3.12	.45	.35	.22	.16	.21	.14	.16	.09
.18	4.39	2.79	.44	.32	.23	.14	.22	.15	.17	.09
.24	6.45	3.90	.43	.17	.22	.07	.21	.10	.19	.11
U = 10 ft/sec										
0.02	8.80	7.80	0.56	0.45	0.24	0.18	0.27	0.21	0.20	0.14
.03	8.00	7.00	.60	.50	.27	.22	.26	.20	.20	.14
.045	7.25	6.20	.64	.55	.28	.24	.25	.20	.19	.14
.06	6.70	5.60	.66	.57	.28	.24	.25	.20	.17	.12
.075	6.45	5.30	.66	.57	.28	.24	.26	.21	.15	.11
.09	6.25	5.05	.64	.55	.27	.23	.26	.21	.14	.11
.12	6.18	4.98	.60	.50	.27	.22	.26	.20	.14	.10
.15	6.30	5.00	.68	.58	.28	.22	.29	.22	.16	.09
.18	6.82	5.22	.80	.68	.29	.20	.32	.25	.19	.11
.24	9.10	6.55	.98	.72	.31	.16	.41	.30	.30	.22

μ	θ = 3.4°									
	$\bar{\beta}$	$\Delta\bar{\beta}$	$\frac{r}{R}$ = 0.25		$\frac{r}{R}$ = 0.42		$\frac{r}{R}$ = 0.625		$\frac{r}{R}$ = 0.833	
			M	ΔM	M	ΔM	M	ΔM	M	ΔM
U = 5 ft/sec										
0.02	3.45	2.45	0.40	0.28	0.19	0.12	0.20	0.07	0.19	0.06
.03	3.85	2.60	.44	.27	.21	.11	.22	.04	.23	.08
.045	4.15	2.75	.49	.25	.23	.09	.24	.04	.23	.07
.06	4.40	2.95	.52	.22	.23	.07	.24	.04	.21	.06
.075	4.40	2.95	.54	.20	.23	.06	.24	.04	.18	.03
.09	4.60	3.05	.55	.19	.23	.06	.23	.04	.17	.03
.12	5.09	3.04	.54	.18	.21	.03	.21	.04	.17	.04
.15	6.05	2.85	.50	.14	.21	.03	.23	.06	.19	.05
.18	7.30	3.05	.55	.16	.22	.04	.27	.10	.22	.07
.24	11.80	7.20	.76	.25	.25	.09	.40	.23	.30	.15
U = 7.5 ft/sec										
0.02	4.40	3.35	0.40	0.28	0.17	0.10	0.18	0.05	0.22	0.09
.03	4.95	3.70	.47	.30	.21	.11	.21	.03	.22	.07
.045	5.30	3.90	.54	.30	.24	.10	.25	.05	.20	.04
.06	5.00	3.55	.59	.29	.26	.10	.26	.06	.18	.03
.075	4.90	3.45	.62	.28	.25	.08	.25	.05	.17	.02
.09	4.95	3.45	.65	.29	.25	.08	.25	.06	.18	.04
.12	6.50	4.45	.65	.29	.24	.06	.26	.09	.20	.07
.15	8.50	5.30	.67	.31	.24	.06	.32	.15	.24	.10
.18	9.95	5.70	.72	.33	.28	.10	.41	.24	.28	.13
.24	12.30	7.70	.89	.38	.45	.29	.46	.29	.36	.21
U = 10 ft/sec										
0.02	6.10	5.05	0.44	0.32	0.22	0.15	0.21	0.08	0.18	0.05
.03	6.50	5.25	.54	.37	.23	.13	.23	.05	.20	.05
.045	6.30	4.90	.61	.37	.25	.11	.25	.05	.21	.05
.06	5.80	4.35	.65	.35	.26	.10	.26	.06	.22	.07
.075	5.90	4.45	.69	.35	.27	.10	.28	.08	.23	.08
.09	6.55	5.00	.71	.35	.28	.11	.29	.10	.23	.09
.12	8.80	6.75	.72	.36	.30	.12	.32	.15	.24	.11
.15	11.09	7.89	.70	.34	.32	.14	.38	.21	.27	.13
.18	12.70	8.45	.74	.35	.33	.15	.43	.28	.31	.16
.24	14.00	9.40	.86	.35	.36	.20	.46	.29	.42	.27

μ	θ = 6.6°									
	$\bar{\beta}$	$\Delta\bar{\beta}$	$\frac{r}{R}$ = 0.25		$\frac{r}{R}$ = 0.42		$\frac{r}{R}$ = 0.625		$\frac{r}{R}$ = 0.833	
			M	ΔM	M	ΔM	M	ΔM	M	ΔM
U = 5 ft/sec										
0.02	4.00	1.80	0.43	0.30	0.20	0.14	0.28	0.16	0.20	0.07
.03	4.98	2.28	.51	.33	.22	.13	.27	.13	.22	.07
.045	6.20	2.80	.53	.29	.23	.11	.27	.11	.24	.09
.06	7.09	2.99	.52	.22	.24	.08	.26	.08	.24	.09
.075	7.40	2.55	.52	.17	.25	.07	.26	.07	.25	.11
.09	8.80	3.20	.52	.13	.26	.06	.25	.04	.25	.12
.12	13.65	6.40	.57	.13	.27	.06	.27	.03	.28	.10
.15	16.35	7.05	.61	.13	.26	.04	.35	.09	.33	.07
.18	18.40	6.65	.63	.12	.25	.03	.38	.10	.35	.07
.24	21.65	6.65	.55	0	.25	.06	.37	.09	.33	.05
U = 7.5 ft/sec										
0.02	5.30	3.10	0.45	0.32	0.21	0.15	0.25	0.13	0.14	0.01
.03	6.30	3.60	.52	.34	.23	.14	.24	.10	.19	.04
.045	7.20	3.80	.54	.30	.25	.13	.25	.09	.24	.09
.06	8.14	4.04	.55	.25	.26	.10	.26	.08	.27	.12
.075	10.10	5.25	.55	.20	.27	.09	.28	.09	.28	.14
.09	12.30	6.70	.56	.17	.27	.07	.30	.09	.29	.16
.12	15.40	8.15	.63	.19	.28	.07	.34	.10	.31	.13
.15	17.85	8.55	.67	.19	.28	.06	.38	.12	.35	.09
.18	19.90	8.15	.68	.17	.28	.06	.41	.13	.39	.11
.24	23.35	8.35	.69	.14	.26	.07	.44	.16	.42	.14
U = 10 ft/sec										
0.02	7.80	5.60	0.47	0.34	0.22	0.16	0.24	0.12	0.20	0.07
.03	8.90	6.20	.49	.31	.21	.12	.23	.09	.22	.07
.045	10.60	7.20	.53	.29	.24	.12	.23	.07	.26	.11
.06	12.20	8.10	.59	.29	.27	.11	.27	.09	.28	.13
.075	13.75	8.90	.65	.30	.28	.10	.32	.13	.30	.16
.09	15.30	9.70	.70	.31	.29	.09	.37	.16	.32	.19
.12	18.15	10.90	.76	.32	.30	.09	.43	.19	.33	.15
.15	20.70	11.40	.79	.31	.30	.08	.46	.20	.38	.12
.18	23.05	11.30	.80	.29	.30	.08	.47	.19	.41	.13
.24	26.60	11.60	.75	.20	.29	.10	.50	.22	.45	.17

TABLE IV.- TABULATION OF BLADE FLAPPING AND BENDING-MOMENT DATA FOR FLAPPING CONFIGURATION (e/R = 0.10)

μ	$\theta = 0.6^\circ$									
	$\bar{\beta}$	$\Delta\bar{\beta}$	$\frac{r}{R} = 0.25$		$\frac{r}{R} = 0.42$		$\frac{r}{R} = 0.625$		$\frac{r}{R} = 0.833$	
			M	ΔM	M	ΔM	M	ΔM	M	ΔM
U = 5 ft/sec										
0.02	2.80	2.20	0.19	0.11	0.08	0.03	0.15	0.08	0.12	0.05
.03	2.80	2.20	.20	.10	.09	.03	.15	.07	.12	.04
.045	2.80	2.20	.22	.09	.11	.04	.16	.06	.13	.04
.06	2.70	2.10	.23	.09	.12	.04	.16	.06	.13	.04
.075	2.60	2.00	.24	.09	.13	.05	.16	.06	.13	.04
.09	2.53	1.93	.25	.10	.14	.06	.17	.07	.13	.04
.12	2.40	1.80	.27	.13	.15	.06	.17	.08	.13	.04
.15	2.50	1.90	.28	.14	.15	.04	.17	.08	.13	.03
.18	2.70	2.10	.30	.14	.16	.05	.17	.08	.14	.04
.24	3.28	2.68	.35	.13	.15	.03	.19	.08	.16	.06
U = 7.5 ft/sec										
0.02	4.95	4.35	0.24	0.16	0.13	0.08	0.17	0.10	0.15	0.08
.03	4.40	3.80	.27	.17	.15	.09	.18	.10	.15	.07
.045	4.00	3.40	.29	.16	.16	.09	.19	.09	.16	.07
.06	3.82	3.22	.32	.18	.17	.09	.19	.09	.17	.08
.075	3.80	3.20	.35	.20	.19	.11	.18	.08	.17	.08
.09	3.80	3.20	.37	.22	.19	.11	.20	.10	.18	.09
.12	3.81	3.21	.42	.28	.21	.12	.23	.14	.18	.09
.15	3.93	3.33	.45	.31	.22	.11	.24	.15	.18	.08
.18	4.18	3.58	.47	.31	.22	.11	.24	.15	.18	.08
.24	5.80	5.20	.48	.26	.23	.11	.22	.11	.17	.07
U = 10 ft/sec										
0.02	7.20	6.60	0.38	0.30	0.18	0.13	0.22	0.15	0.21	0.14
.03	6.85	6.25	.36	.26	.20	.14	.23	.15	.20	.12
.045	6.40	5.80	.35	.22	.21	.14	.23	.13	.18	.09
.06	6.00	5.40	.38	.24	.21	.13	.22	.12	.16	.07
.075	5.70	5.10	.42	.27	.22	.14	.19	.09	.16	.07
.09	5.50	4.90	.47	.32	.22	.14	.19	.09	.19	.10
.12	5.37	4.77	.49	.35	.23	.14	.20	.11	.21	.12
.15	5.60	5.00	.50	.36	.24	.13	.24	.15	.22	.12
.18	6.40	5.80	.49	.33	.26	.15	.28	.19	.22	.12
.24	11.00	10.40	.45	.23	.30	.18	.40	.29	.19	.09

μ	$\theta = 3.4^\circ$									
	$\bar{\beta}$	$\Delta\bar{\beta}$	$\frac{r}{R} = 0.25$		$\frac{r}{R} = 0.42$		$\frac{r}{R} = 0.625$		$\frac{r}{R} = 0.833$	
			M	ΔM	M	ΔM	M	ΔM	M	ΔM
U = 5 ft/sec										
0.02	3.30	1.85	0.34	0.22	0.20	0.11	0.24	0.10	0.28	0.15
.03	3.70	1.90	.40	.23	.23	.10	.27	.09	.29	.13
.045	4.20	2.10	.42	.19	.25	.07	.27	.04	.26	.09
.06	4.38	2.18	.43	.15	.25	.05	.27	.02	.22	.04
.075	4.50	2.25	.42	.11	.24	.03	.25	.01	.19	.01
.09	4.50	2.25	.40	.09	.22	.02	.23	.01	.17	0
.12	4.70	2.40	.36	.06	.19	.01	.20	.01	.16	-.01
.15	5.10	2.65	.33	.05	.18	0	.20	.01	.16	-.03
.18	5.70	2.40	.35	.06	.19	0	.22	.03	.17	-.02
.24	8.38	4.18	.47	.05	.20	0	.26	.03	.18	0
U = 7.5 ft/sec										
0.02	4.50	3.05	0.32	0.20	0.17	0.08	0.21	0.07	0.23	0.10
.03	4.94	3.14	.39	.22	.21	.08	.24	.06	.25	.09
.045	5.00	2.90	.43	.20	.23	.05	.26	.03	.25	.08
.06	5.05	2.85	.45	.17	.25	.05	.26	.01	.24	.06
.075	5.05	2.80	.45	.14	.24	.03	.25	.01	.22	.04
.09	5.10	2.85	.45	.14	.22	.02	.23	.01	.20	.03
.12	5.35	3.05	.43	.13	.22	.04	.24	.05	.18	.01
.15	6.00	4.15	.41	.13	.24	.06	.28	.09	.18	-.01
.18	8.40	5.10	.40	.11	.26	.07	.31	.12	.20	.01
.24	9.85	5.65	.52	.10	.29	.09	.36	.13	.26	.08
U = 10 ft/sec										
0.02	5.75	4.30	0.31	0.19	0.17	0.08	0.20	0.06	0.22	0.09
.03	6.18	4.38	.39	.22	.20	.07	.24	.06	.23	.07
.045	6.20	4.10	.46	.23	.23	.05	.26	.03	.25	.08
.06	6.20	4.00	.49	.21	.24	.04	.27	.02	.26	.08
.075	6.25	4.00	.51	.20	.25	.04	.28	.04	.26	.08
.09	6.58	4.33	.52	.21	.26	.06	.29	.07	.26	.09
.12	8.67	6.37	.50	.20	.25	.07	.30	.11	.25	.08
.15	11.18	8.73	.47	.19	.25	.07	.33	.14	.26	.07
.18	12.85	9.55	.48	.19	.26	.07	.38	.19	.29	.10
.24	14.20	10.00	.59	.17	.31	.11	.49	.26	.40	.22

μ	$\theta = 6.6^\circ$									
	$\bar{\beta}$	$\Delta\bar{\beta}$	$\frac{r}{R} = 0.25$		$\frac{r}{R} = 0.42$		$\frac{r}{R} = 0.625$		$\frac{r}{R} = 0.833$	
			M	ΔM	M	ΔM	M	ΔM	M	ΔM
U = 5 ft/sec										
0.02	4.50	2.05	0.41	0.23	0.26	0.15	0.32	0.15	0.27	0.09
.03	5.40	2.20	.49	.28	.31	.16	.36	.16	.33	.14
.045	6.25	2.30	.50	.25	.31	.11	.38	.15	.35	.16
.06	6.85	2.25	.47	.19	.28	.05	.34	.09	.32	.13
.075	8.00	2.80	.45	.13	.27	.02	.30	.03	.29	.09
.09	9.90	4.10	.45	.09	.27	.01	.29	0	.28	.05
.12	14.90	7.90	.50	.05	.28	.02	.37	.05	.31	-.02
.15	17.90	9.40	.58	.04	.30	.04	.43	.09	.38	-.05
.18	20.10	7.60	.62	0	.32	.05	.47	.10	.42	-.05
.24	23.25	5.15	.67	-.06	.36	.06	.53	.11	.48	.02
U = 7.5 ft/sec										
0.02	6.10	3.65	0.38	0.20	0.22	0.11	0.29	0.12	0.20	0.02
.03	6.70	3.50	.45	.24	.23	.08	.32	.12	.27	.08
.045	8.00	4.05	.49	.24	.26	.06	.32	.09	.30	.11
.06	9.85	5.25	.48	.20	.27	.04	.31	.06	.29	.10
.075	12.20	7.00	.46	.14	.28	.03	.32	.05	.30	.10
.09	14.30	8.50	.47	.11	.30	.04	.35	.06	.32	.09
.12	17.87	10.87	.51	.06	.32	.06	.39	.07	.37	.04
.15	20.40	11.90	.55	.01	.34	.08	.44	.10	.42	-.01
.18	22.30	9.80	.59	-.03	.37	.10	.48	.11	.46	-.01
.24	25.27	7.17	.67	-.06	.40	.10	.58	.16	.55	.09
U = 10 ft/sec										
0.02	8.90	6.45	0.44	0.26	0.30	0.19	0.33	0.16	0.29	0.11
.03	10.40	7.20	.45	.24	.30	.15	.32	.12	.30	.11
.045	12.50	8.55	.46	.21	.29	.09	.31	.08	.29	.10
.06	14.50	9.90	.46	.18	.28	.05	.33	.08	.28	.09
.075	16.30	11.10	.47	.15	.28	.03	.35	.08	.32	.12
.09	17.95	12.15	.48	.12	.31	.05	.39	.10	.36	.13
.12	20.85	13.85	.56	.11	.36	.10	.48	.16	.43	.10
.15	23.30	14.80	.63	.09	.39	.13	.55	.21	.50	.07
.18	25.25	12.75	.68	.06	.41	.14	.62	.25	.54	.07
.24	28.50	10.40	.73	0	.44	.14	.71	.29	.58	.12

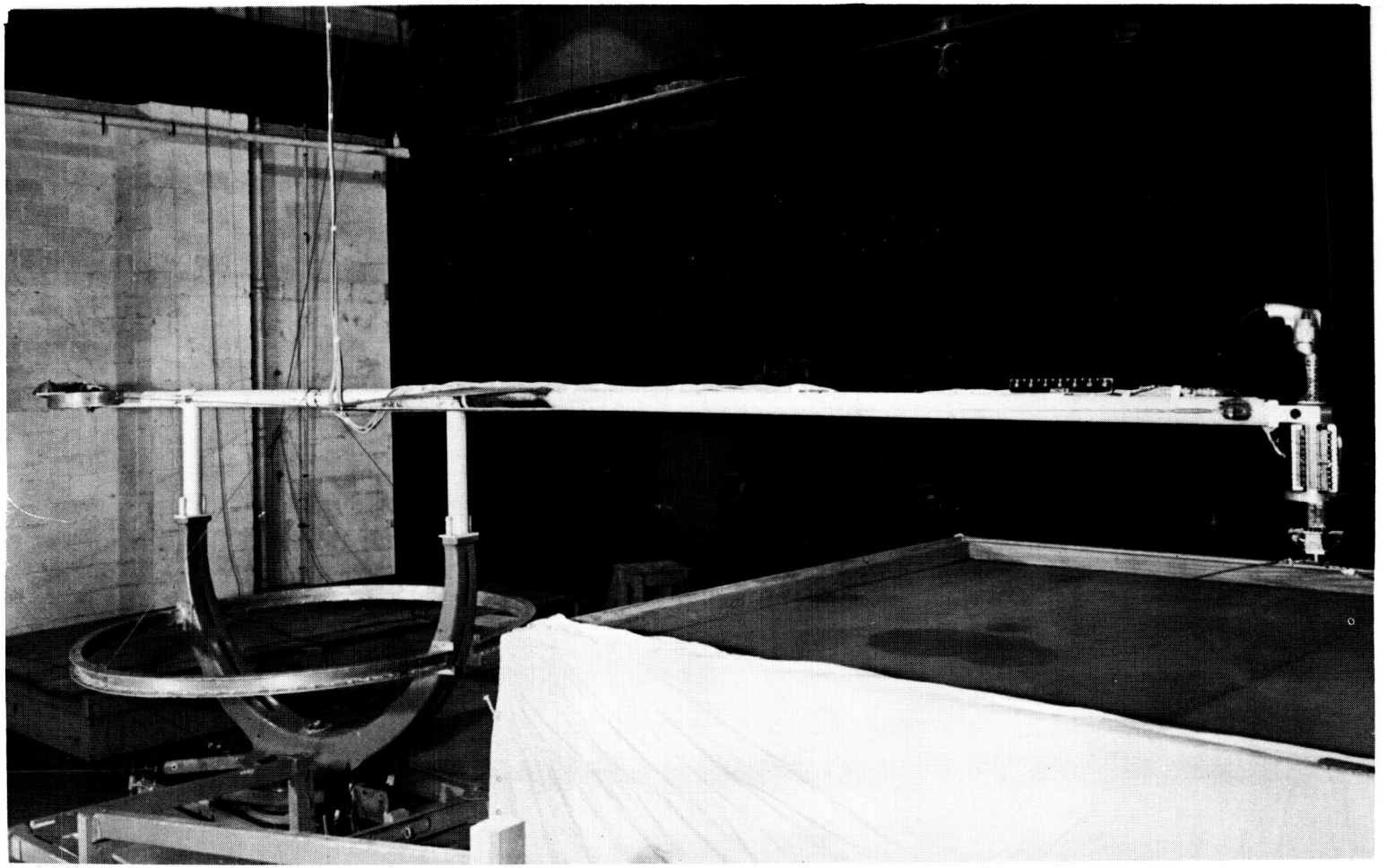

Figure 1.- Photograph of test apparatus. L-58-3309

L-58-3311

Figure 2.- Close-up of rotor assembly mounted to whirling arm.

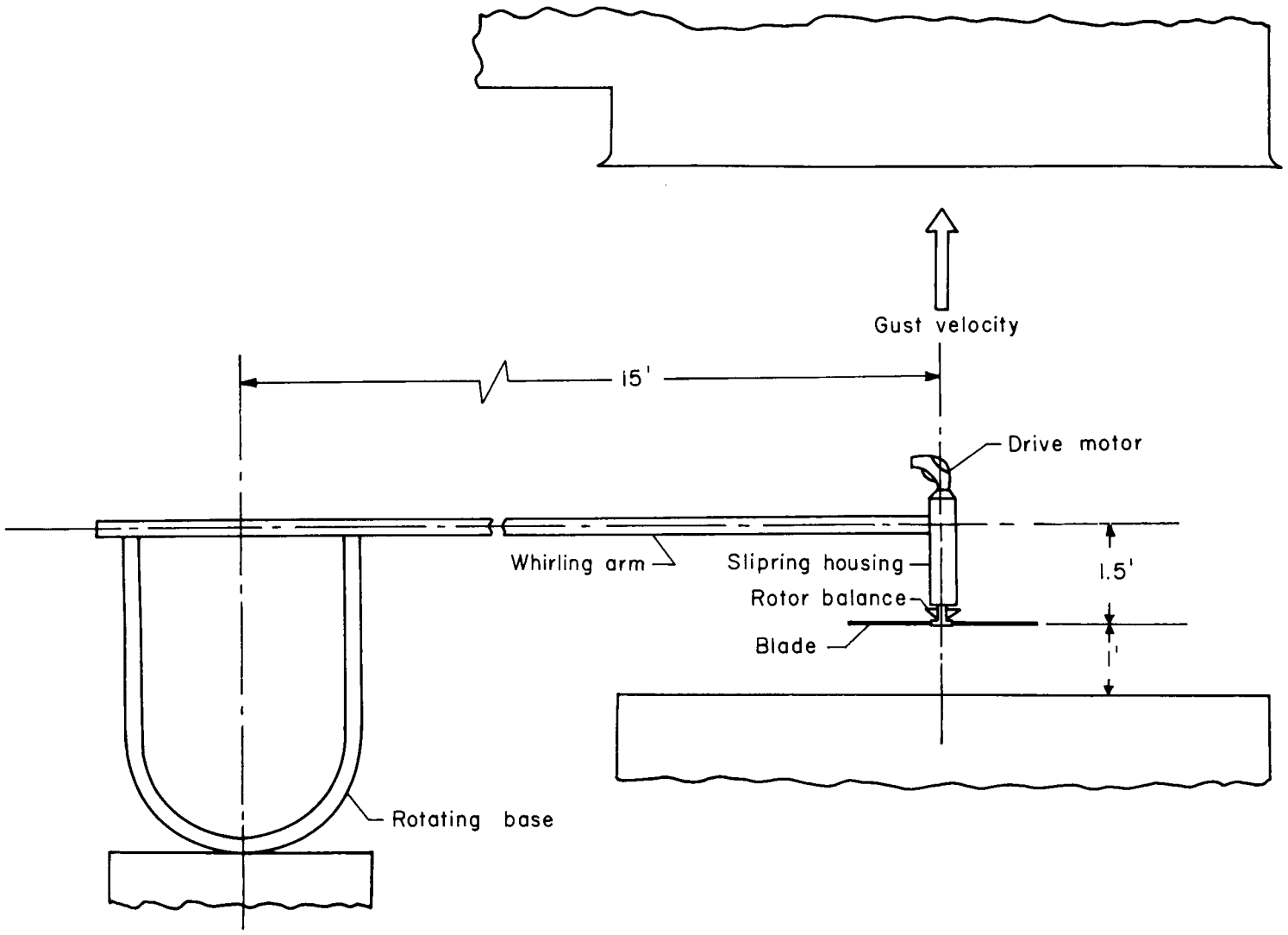

Figure 3.- Sketch of test apparatus.

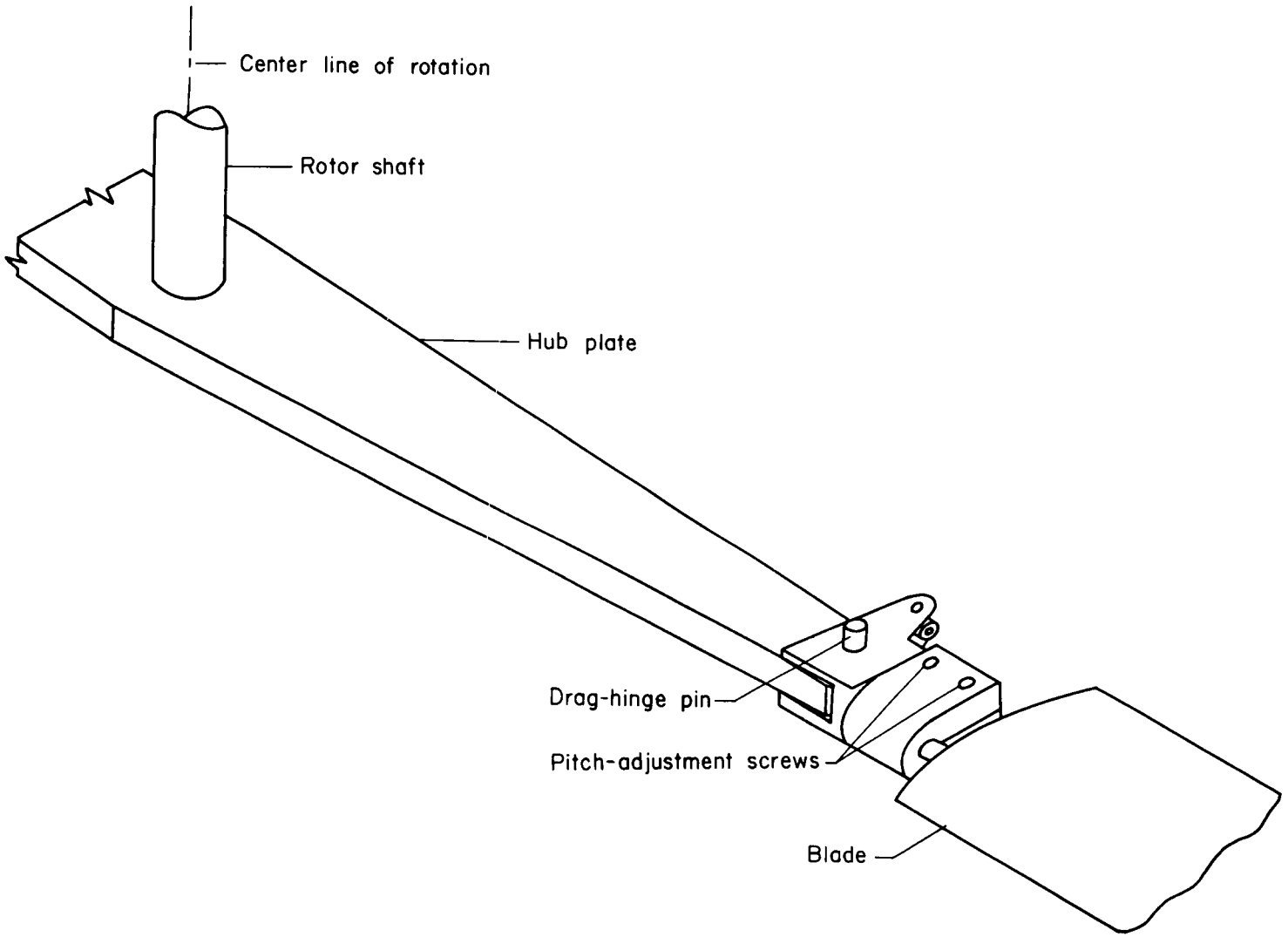

Figure 4.- Sketch of blade root fitting for fixed-at-root configuration.

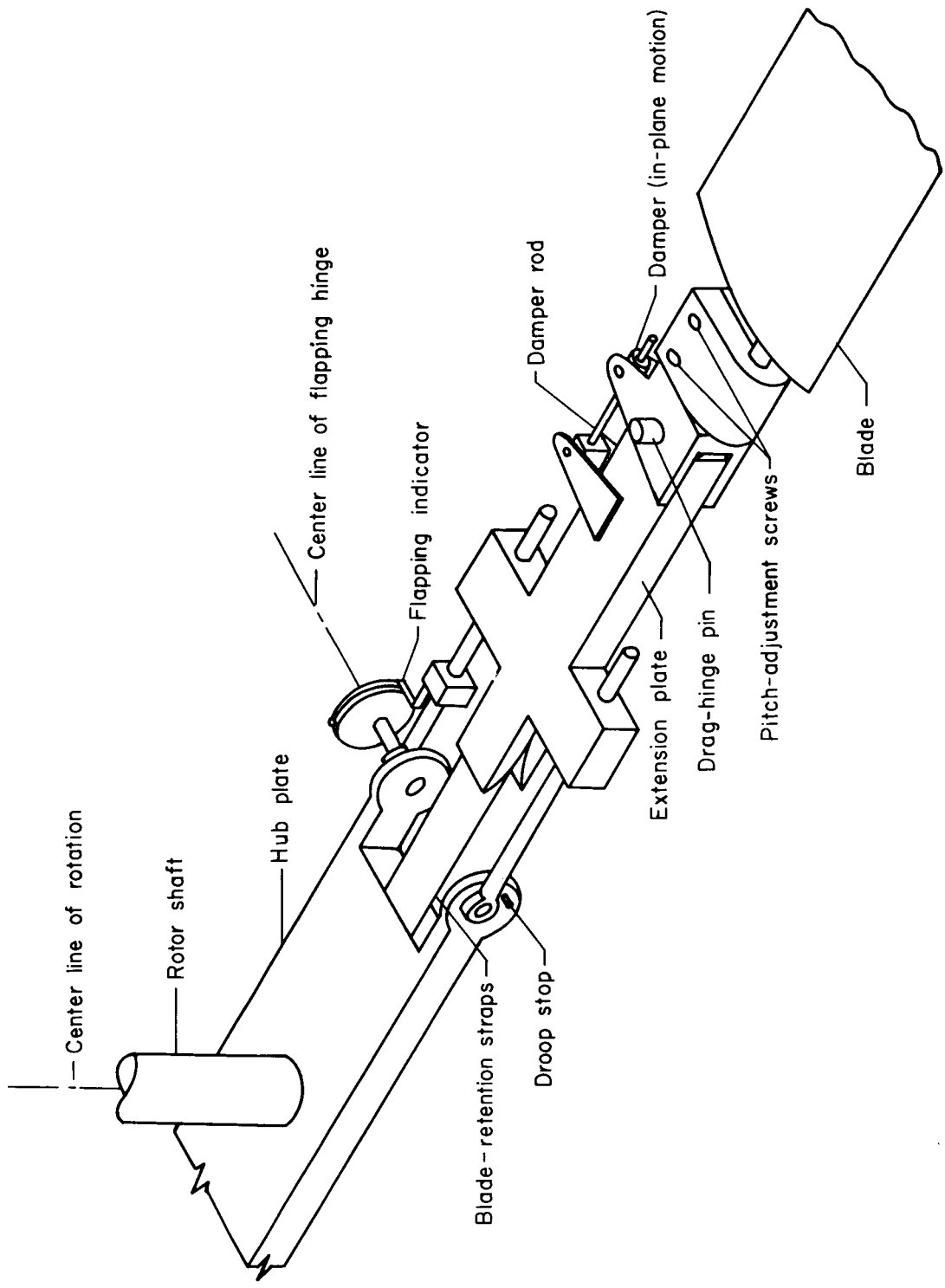

Figure 5.- Sketch of blade root fitting for flapping configuration.

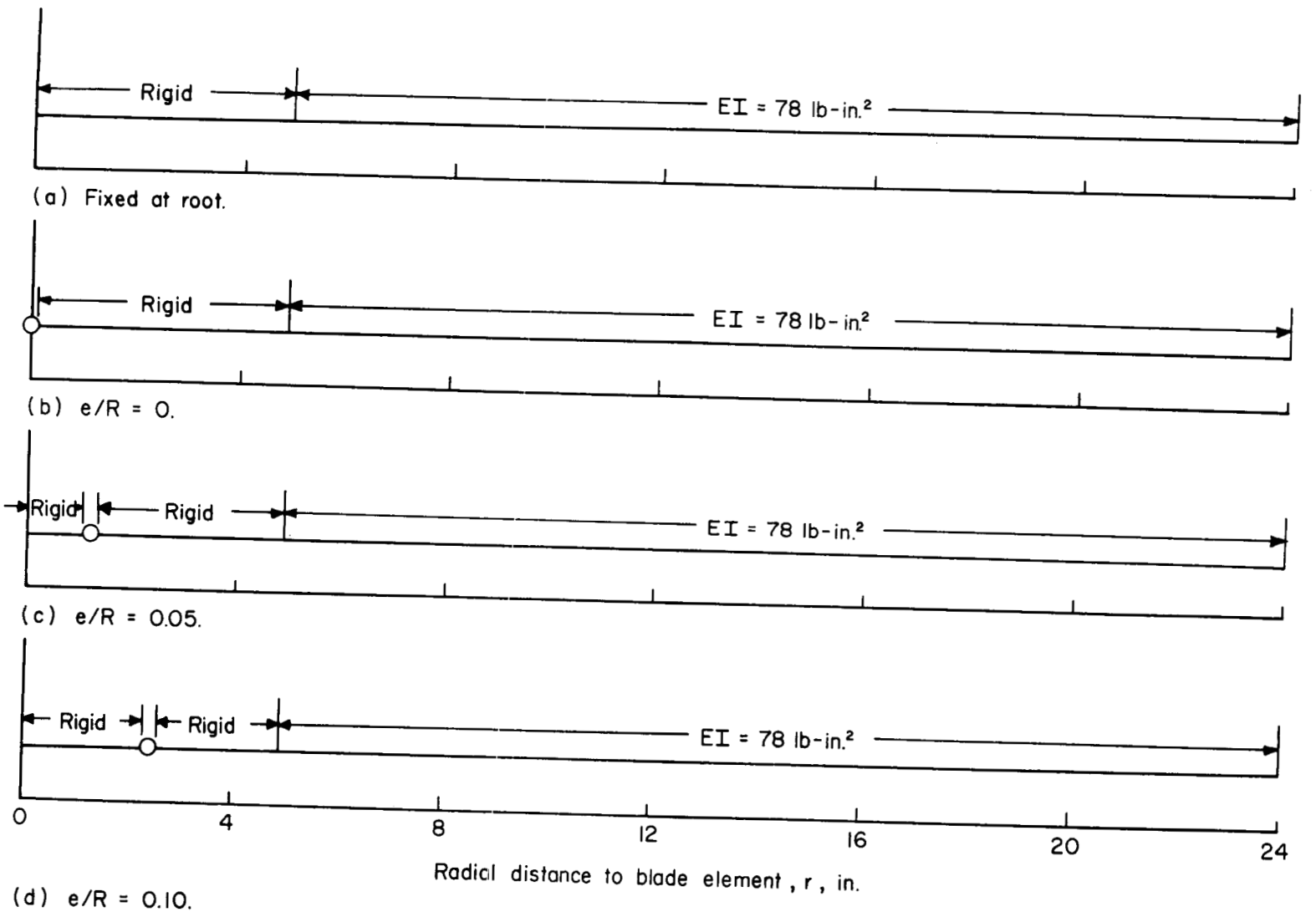

Figure 6.- Blade spanwise stiffness distribution for the different root configurations.

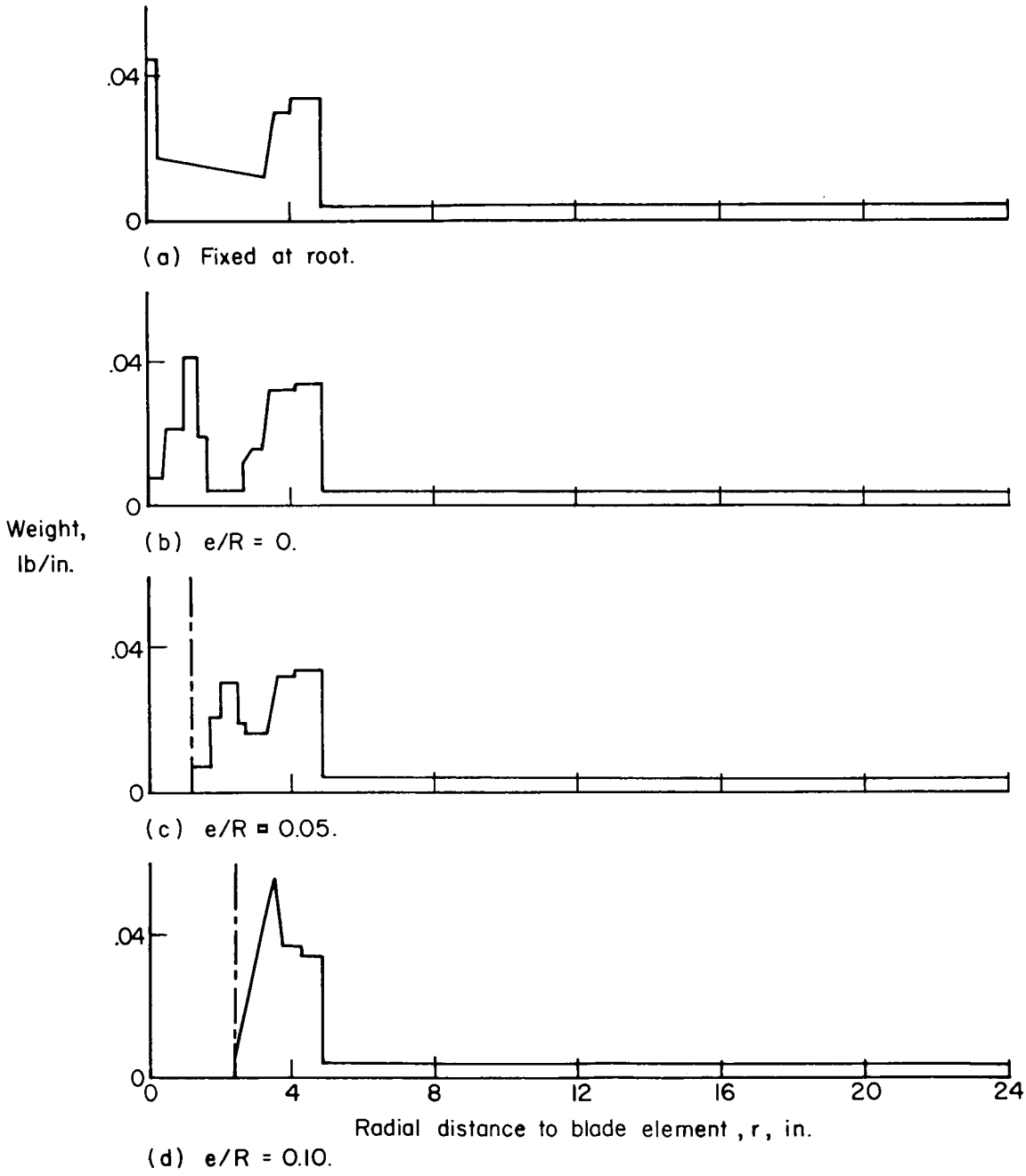

Figure 7.- Blade spanwise weight distributions for the different root configurations.

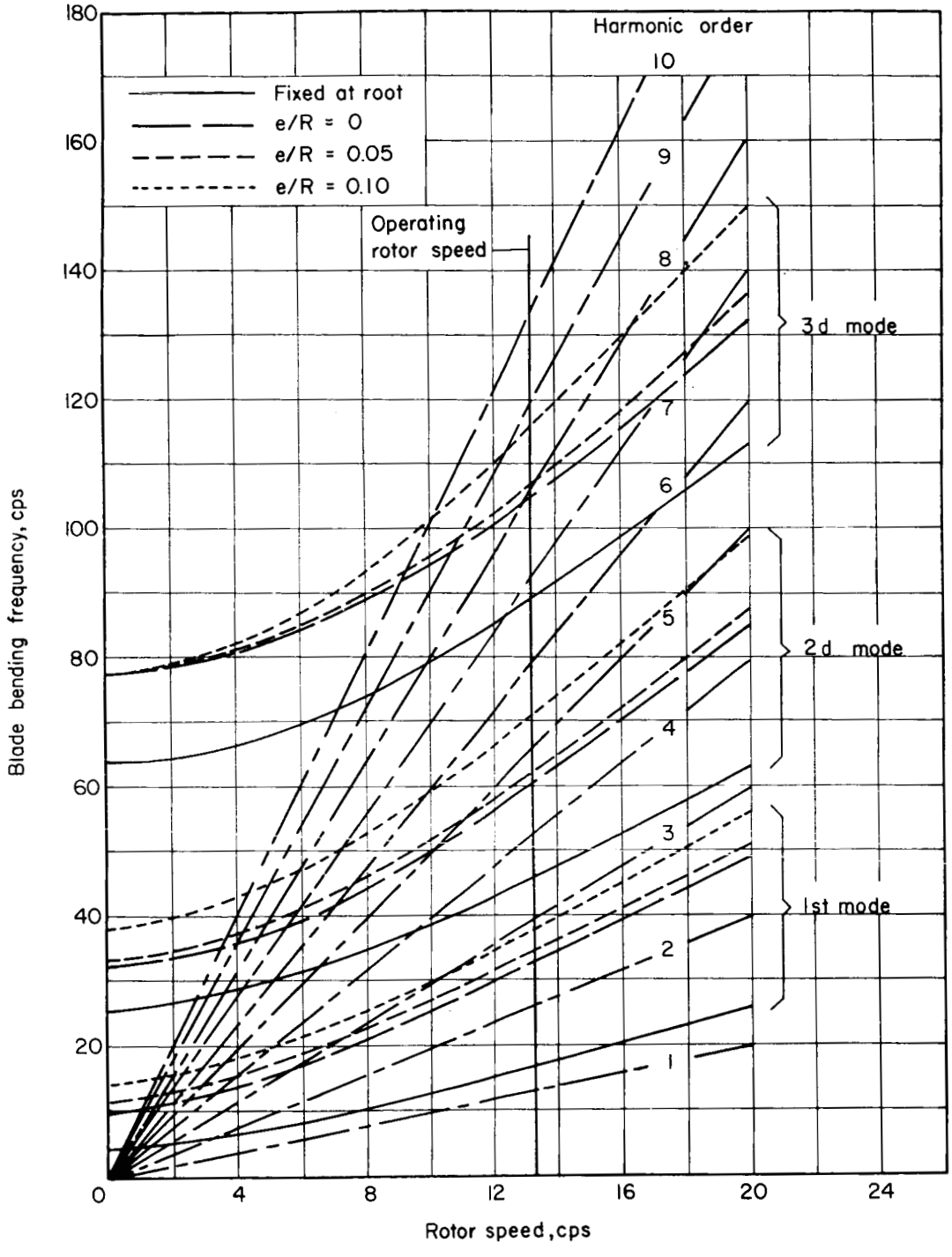

Figure 8.- Variation of blade bending frequency with rotor speed for the first 3 modes and for the various root configurations.

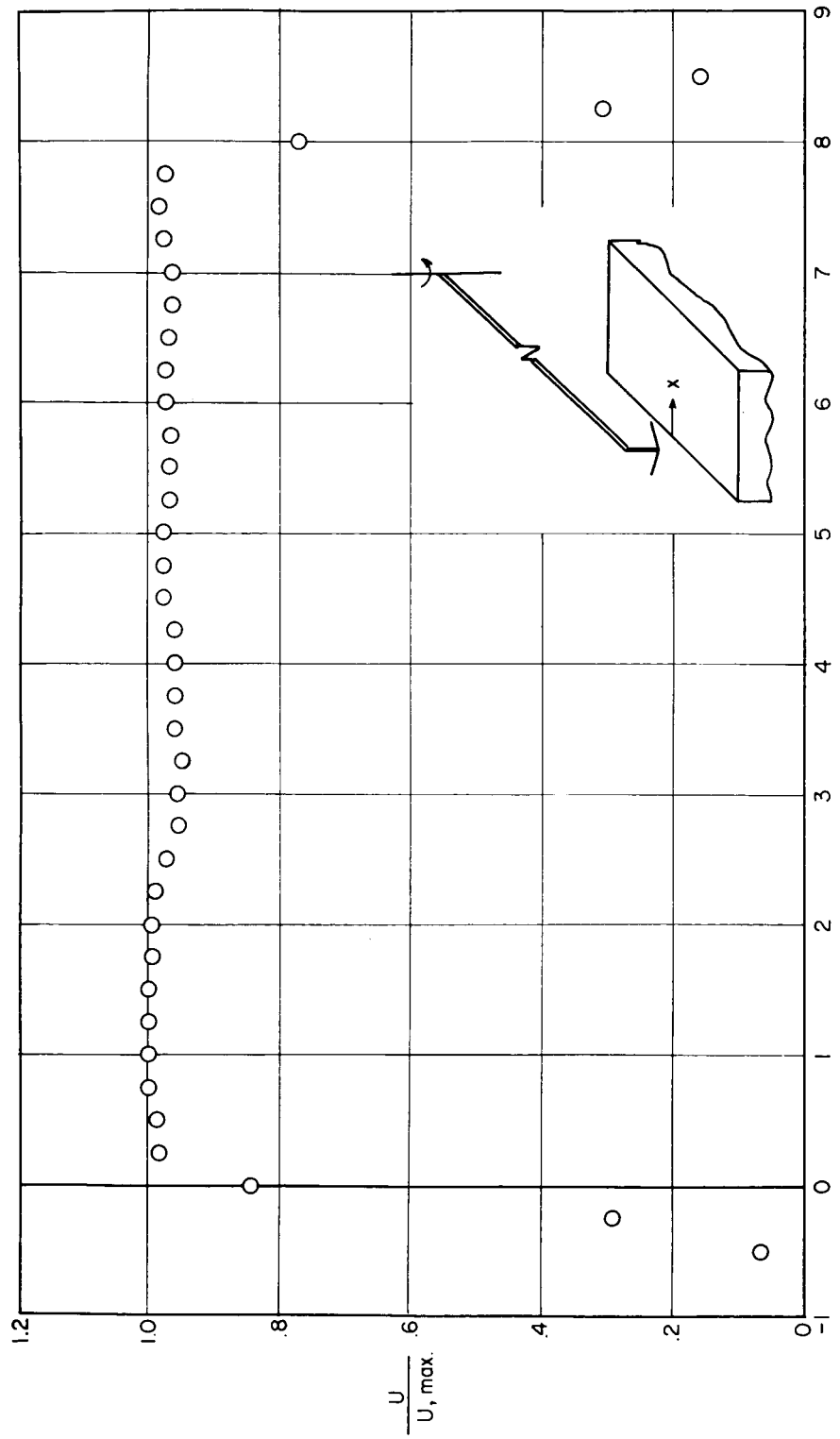

Figure 9.- Cross survey of gust tunnel in plane of rotor. (U_{max} = 10 fps).

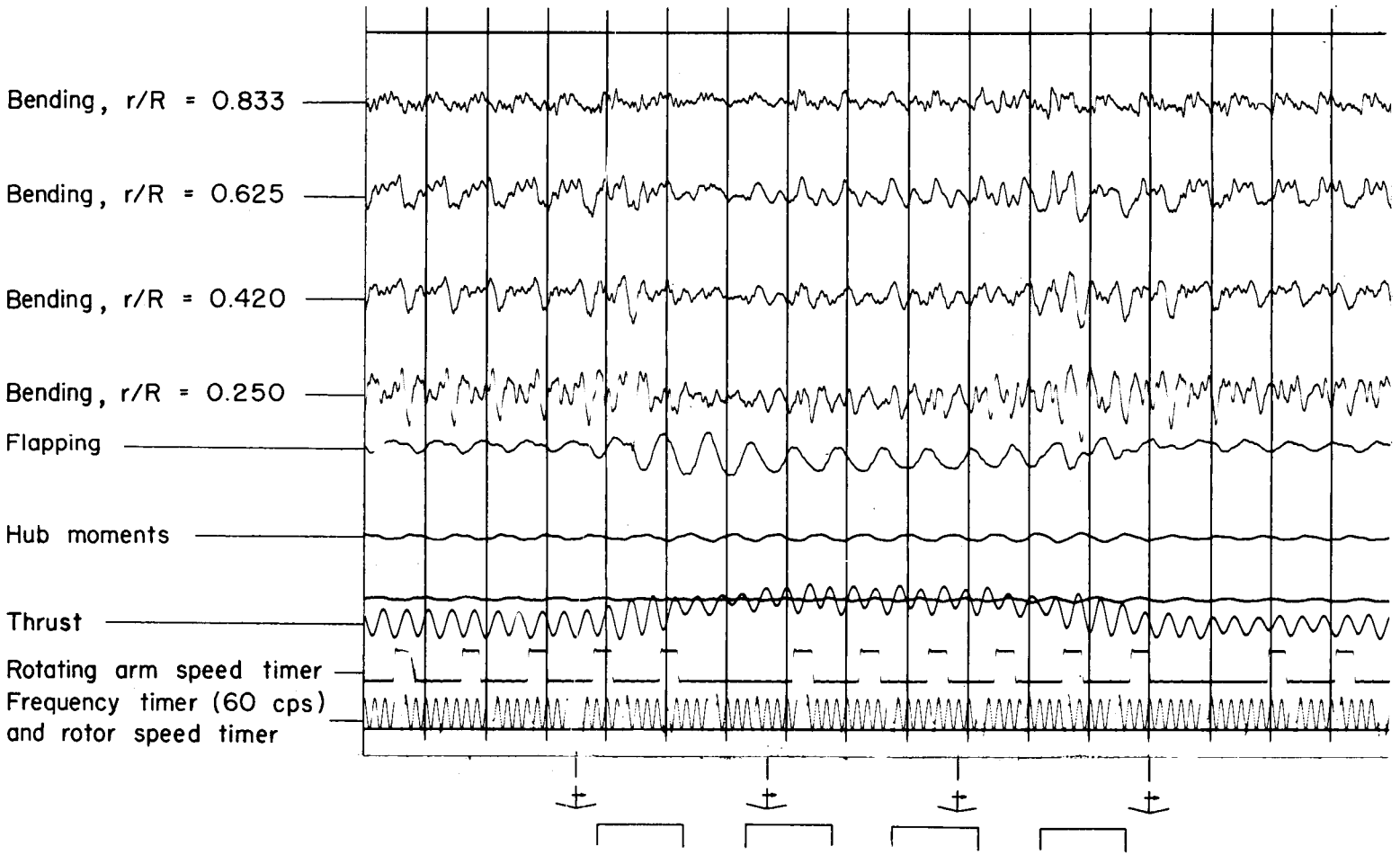

Figure 10.- Section of typical oscillograph record with schematic showing position of rotor relative to the tunnel.

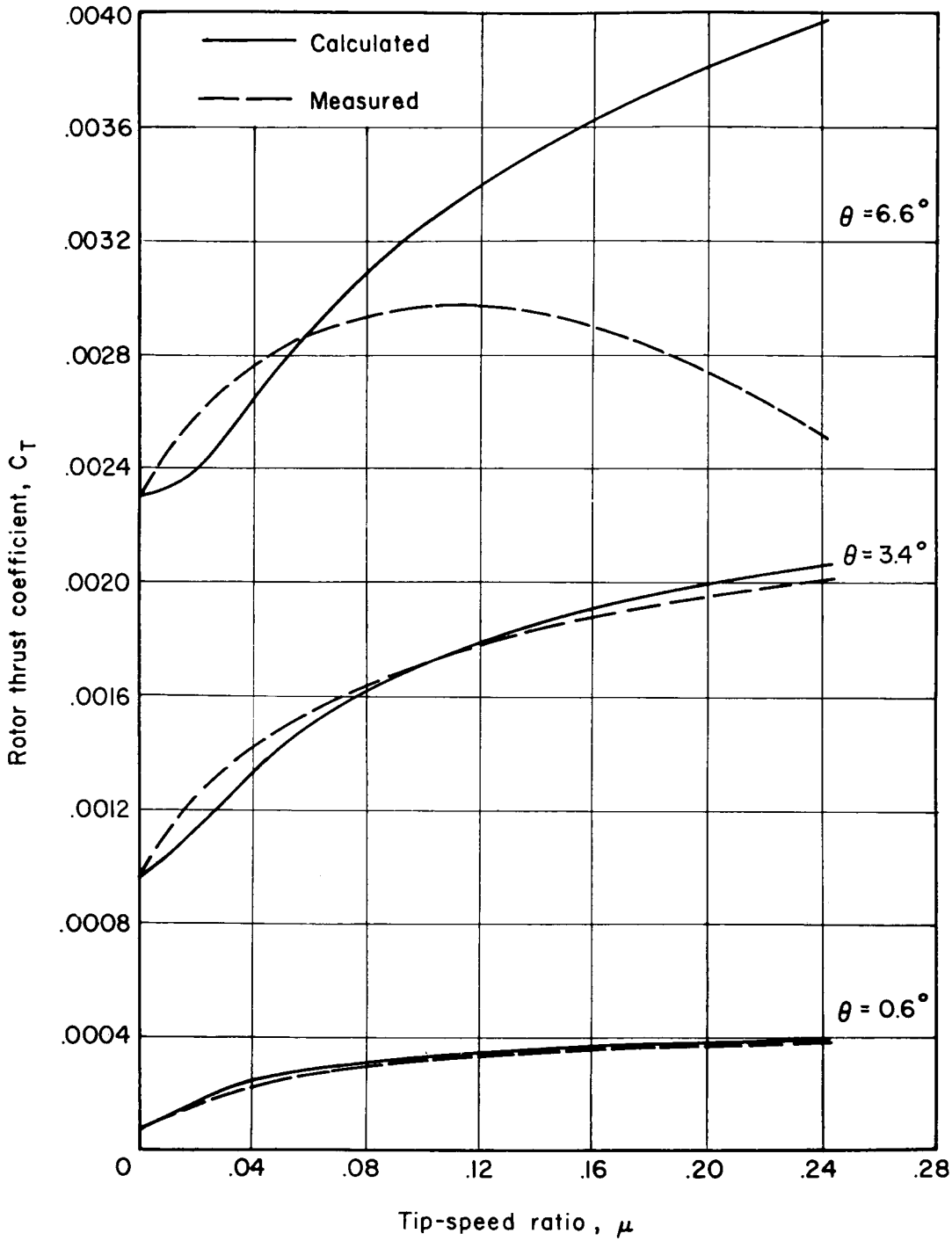

Figure 11.- Comparison of calculated and measured rotor thrust coefficients.

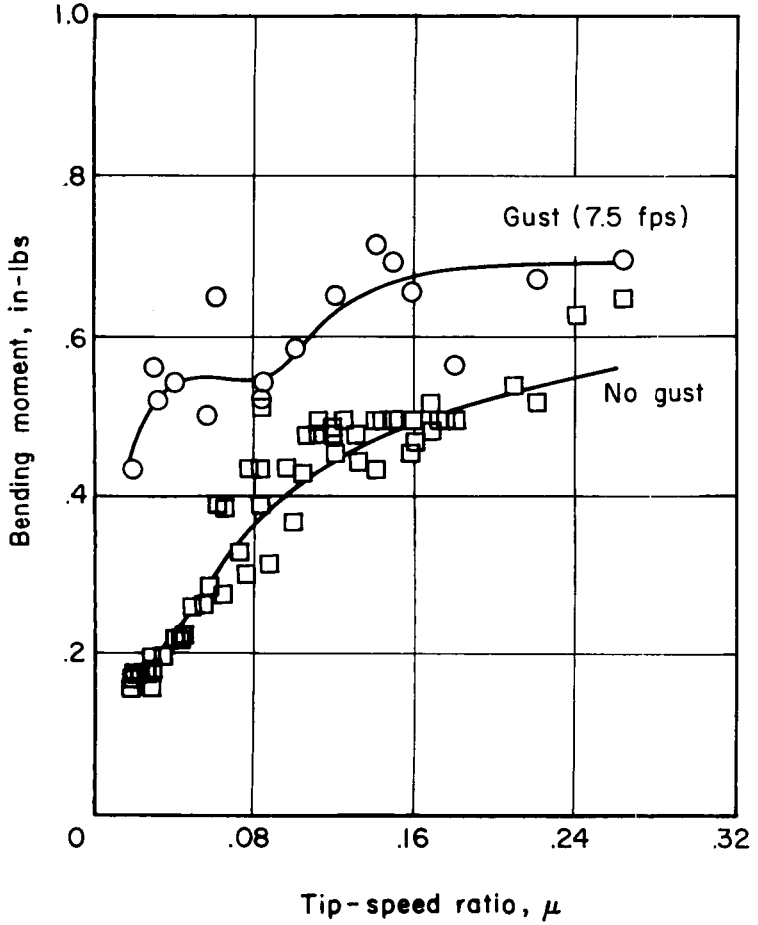

(a) Bending moment, r/R = 0.25.

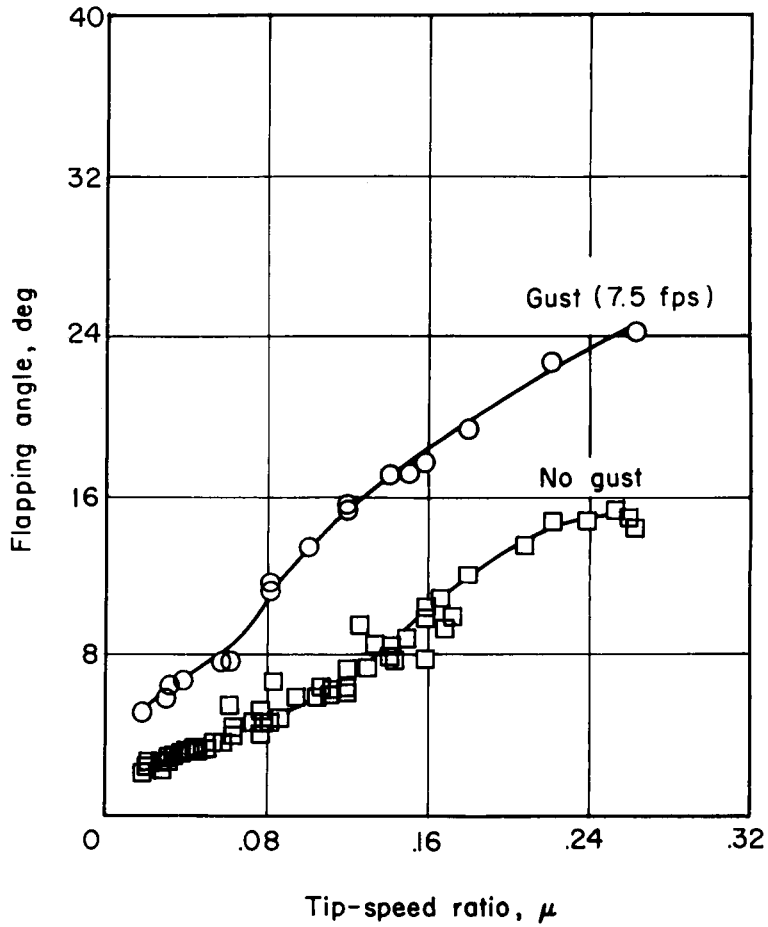

(b) Flapping angle.

Figure 12.- Typical variation of double-amplitude blade bending moments and flapping angles with tip-speed ratio. (e/R = 0.05; θ = 6.6°.)

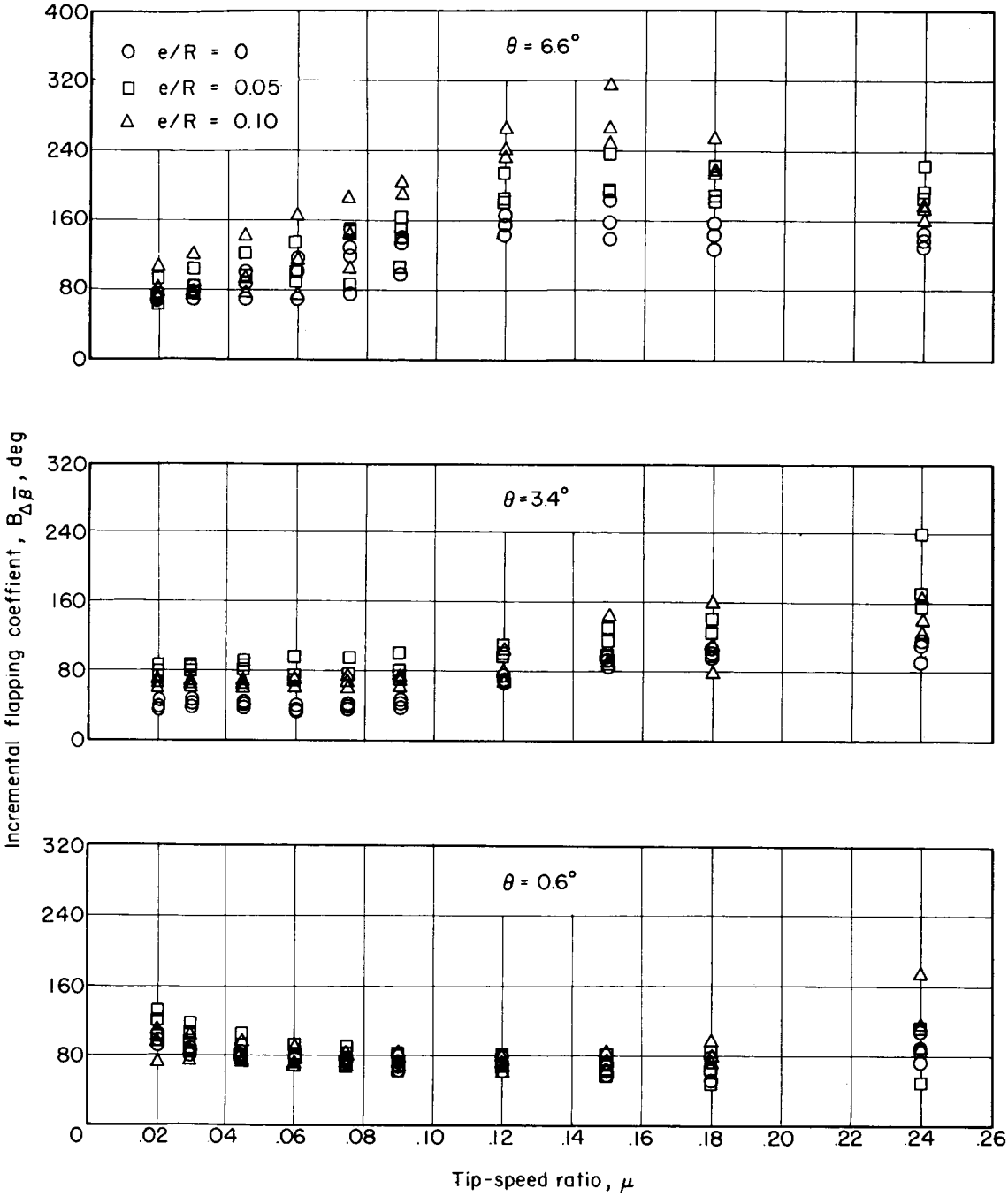

Figure 13.- Variation of flapping coefficient with tip-speed ratio for three collective pitch angle settings.

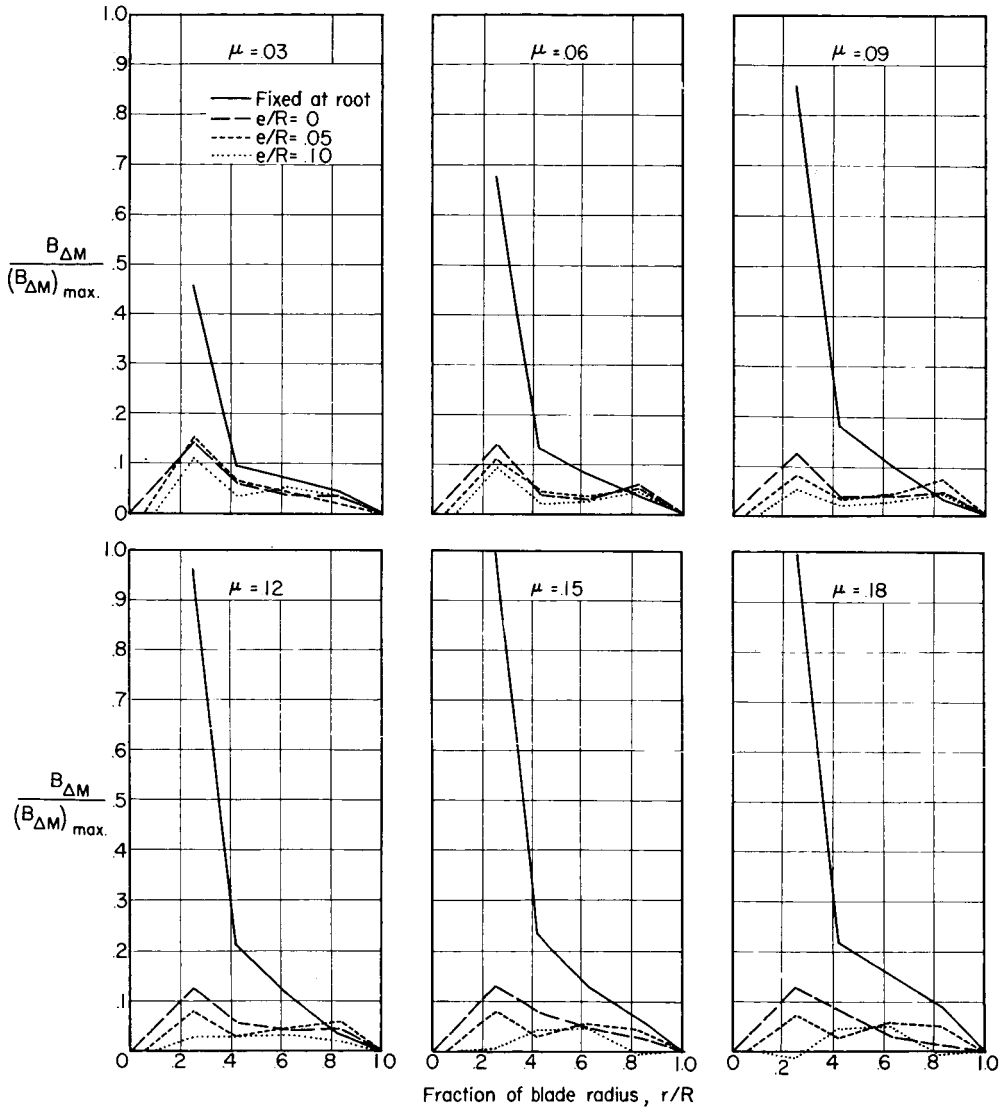

Figure 14.- Spanwise distribution of incremental bending-moment coefficient at $\theta = 6.6^{o}$ and $U = 75$ ft/sec $\left(B_{\Delta M_{max}} = 0.1321\right)$.

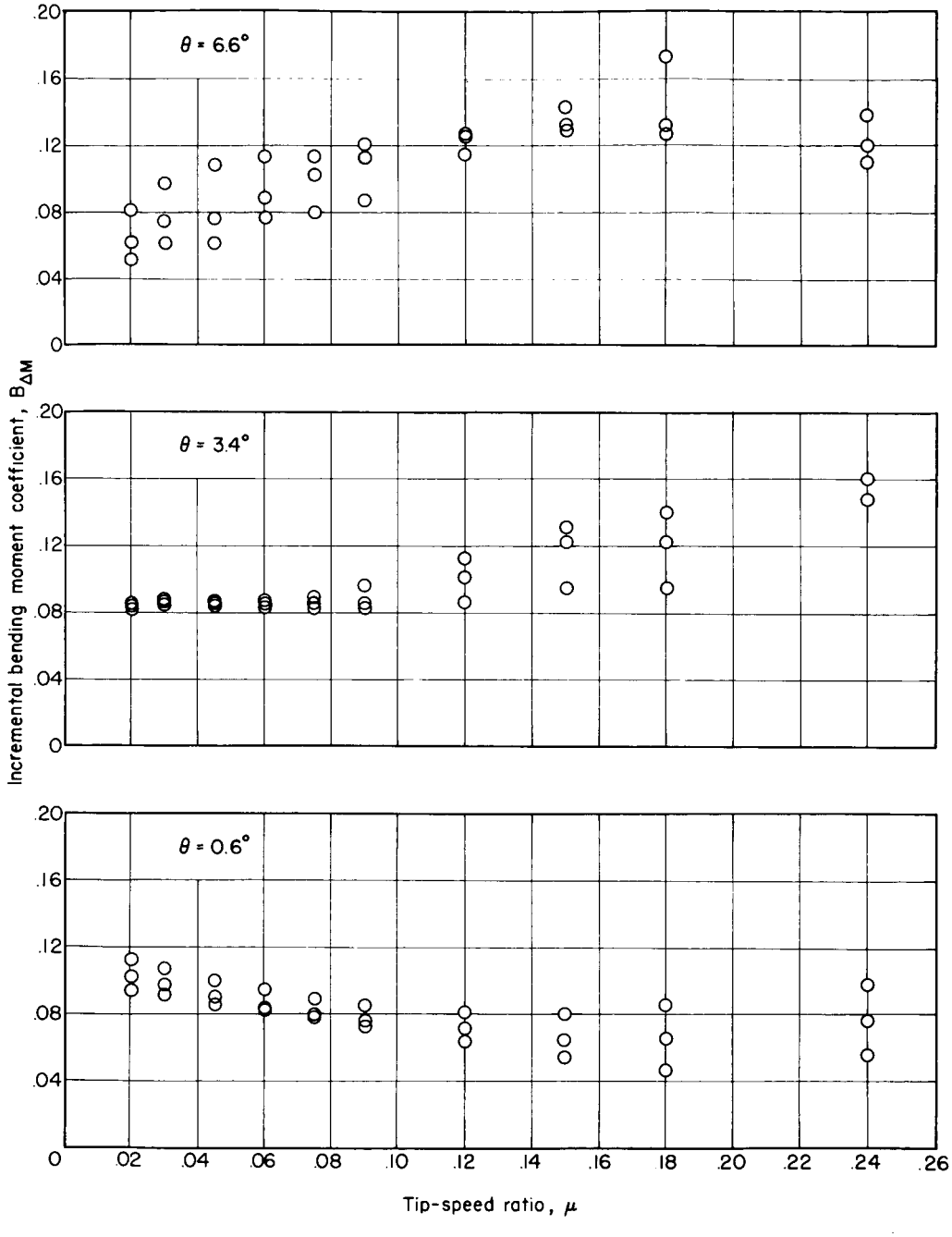

Figure 15.- Variation of incremental bending-moment coefficient at r/R = 0.25 with tip-speed ratio for the fixed-at-root configuration at three collective pitch angle settings.

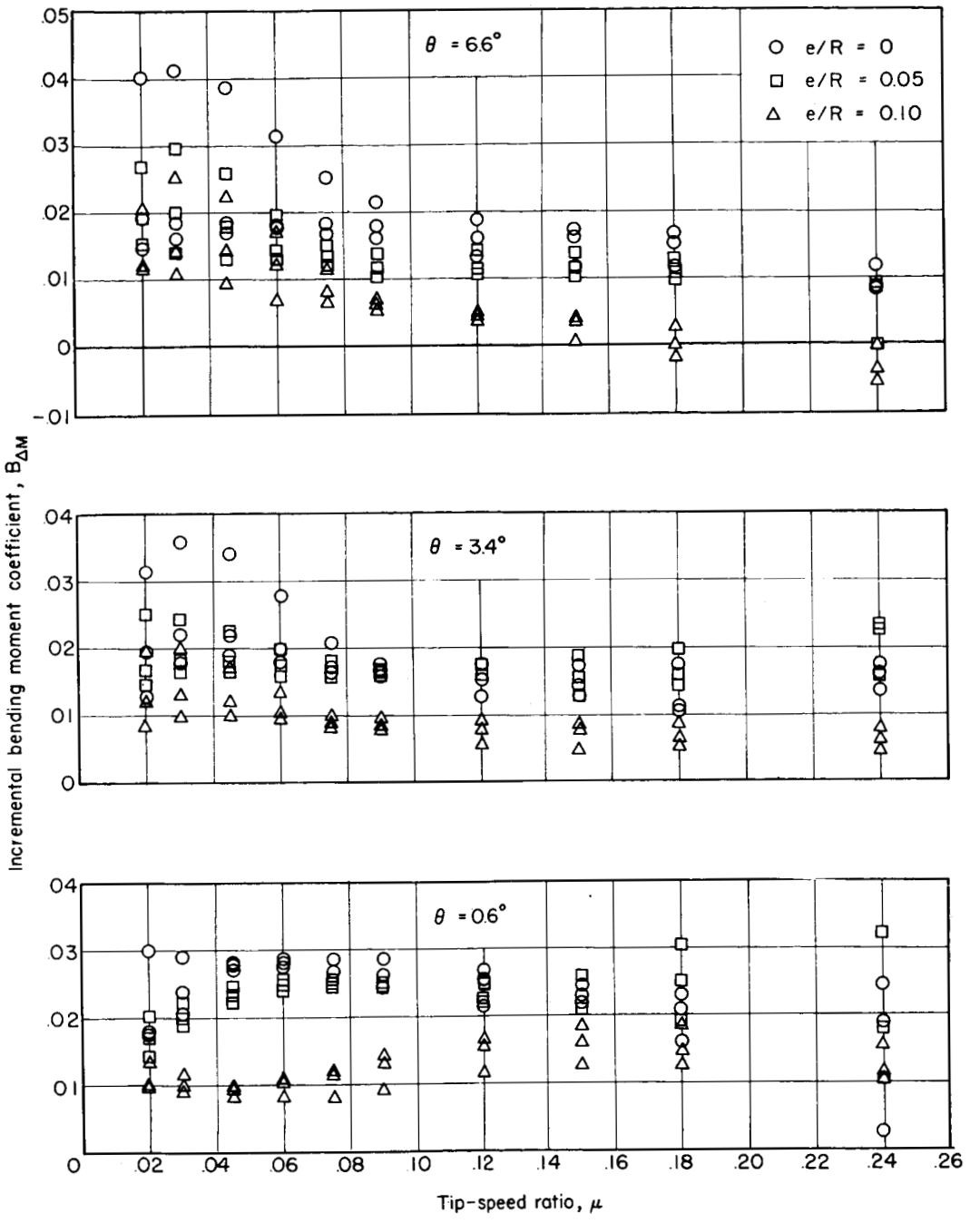

Figure 16.- Variation of incremental bending-moment coefficient at r/R = 0.25 with tip-speed ratio for the flapping configurations at three collective pitch angle settings.